1.0

1.1

1.25

4.5
5.0

2.8
3.2
3.6
4.0

2.5
2.2
2.0
1.8

1.4

1.6

MICROCOPY RESOLUTION TEST CHART
NATIONAL BUREAU OF STANDARDS-1963-A

ONE-DIMENSIONAL ANALYSIS OF
SALINITY INTRUSION IN ESTUARIES

by

Arthur T. Ippen and Donald R. F. Harleman

LEVEL

TECHNICAL BULLETIN NO. 5

June 1961

Committee on Tidal Hydraulics

CORPS OF ENGINEERS, U. S. ARMY

80   1 23 064

REPORTS OF COMMITTEE ON TIDAL HYDRAULICS

ONE-DIMENSIONAL ANALYSIS OF SALINITY INTRUSION IN ESTUARIES.

by

Arthur T. Ippen and Donald R. F. Harleman

Committee on Tidal Hydraulics

CORPS OF ENGINEERS, U. S. ARMY

PREFACE

An analytical investigation of salinity intrusions and related phenomena was initiated by the Corps of Engineers Committee on Tidal Hydraulics in January 1954. The objectives of the investigation were stated by the Committee at its 21st meeting at Vicksburg, Mississippi, in January 1955:

> "The present broad purpose of the investigation is to determine the effects of the physical and hydraulic features of estuaries (such as tidal prism, tidal range, fresh-water discharge, channel depth, channel width, etc.) on the extent of salinity intrusion, the nature of salinity intrusion, the magnitudes and durations of current velocities, and other factors considered essential to proper solution of estuarine problems encountered by the Corps of Engineers."

The experimental portion of the investigation was conducted at the U. S. Army Engineer Waterways Experiment Station (Civil Works Investigation Item CW 843) under the immediate supervision of Mr. Henry B. Simmons, Chief, Estuaries Section. All of the experimental data presented and analyzed in this report were obtained in the Waterways Experiment Station rectangular salinity flume and were forwarded to the authors of this report during the period between September 1955 and November 1959. The analytical part of the study was carried out by the authors, Dr. Arthur T. Ippen and Dr. Donald R. F. Harleman, at the Hydrodynamics Laboratory, Massachusetts Institute of Technology, under contract DA-22-079-eng-158.

The general investigation is designed to cover the following four phases:*

---

* Minutes of the 34th Meeting of the Committee on Tidal Hydraulics, June 1959.

a. The extent of salinity intrusion and the mean salinity
　　　　distribution.

　　　b. The vertical mixing of fresh and salt water and the result-
　　　　ing vertical salinity distribution.

　　　c. The vertical distribution of current velocities as affected
　　　　by salinity distribution.

　　　d. The movement and deposition of sediments as affected by
　　　　density-current phenomena.

This report is primarily concerned with the first phase, a one-dimensional
treatment of salinity intrusion in a partially or well-mixed type of
estuary.

　　　In June 1957 the authors submitted a preliminary report to the Com-
mittee on Tidal Hydraulics which defined and verified the basic analytical
procedures. This resulted in an expanded experimental program to test the
conclusions reached at that time. The present report should be considered
as superseding the previous report in view of the more comprehensive ex-
perimental program and conclusions now available.

ACKNOWLEDGMENT

CONTENTS

NOTATIONS

a   Tidal amplitude in ocean, ft

A_o Amplitude of incident and reflected waves at closed end of estuary, ft

b   Width of estuary, ft

B   Seaward excursion to point where salinity is constant throughout tidal cycle, ft

c   Tidal wave celerity, ft/sec

c_o Frictionless tidal wave celerity, ft/sec

D   Turbulent diffusion coefficient, ft^2/sec

D'   Apparent diffusion coefficient, ft^2/sec (subscript o indicates diffusion coefficient at ocean entrance)

E   Tidal wave energy per unit surface area, lb/ft

g   Acceleration of gravity, ft/sec^2

G   Rate of tidal energy dissipation per unit mass of fluid, ft^2/sec^3

h   Mean water depth, ft

J   Rate of gain of potential energy per unit mass of fluid, ft^2/sec^3

k   Wave number, $2\pi/\lambda$

ℓ Mean eddy size, ft

L   Length of estuary, ft

L_m Minimum salinity-intrusion length, ft

L_t Maximum salinity-intrusion length, ft

n   Manning's roughness

P   Energy flux (power), ft-lb/sec

P_t Tidal prism, ft^3

Q_f Fresh-water discharge into estuary, ft^3/sec

s   Salinity concentration, ppt

s_o Salinity concentration in ocean, ppt

t Time, sec

t_H Local time of high water

t_M Local time of maximum velocity

T Tidal period, sec

u Tidal velocity in x direction, ft/sec

u_o Maximum tidal velocity at ocean entrance, ft/sec

U Velocity of fresh-water flow, ft/sec

v Velocity in y direction, ft/sec

w Velocity in z direction, ft/sec

W $U/2D_o'B$

x Longitudinal direction, ft

y Vertical direction, ft

z Width direction, ft

α $\text{Tan}^{-1}(\phi/2\pi)$

β Dimensionless time interval, t/T

γ Specific weight of fluid, lb/ft^3

ΔD Mass-transfer coefficient due to gravitational convection, ft^2/sec

δ $a\sigma/hu_o$

η Tidal wave elevation above or below mean sea level, ft

η_H Local high water, ft

η_{oH} High water at closed end of estuary, ft

θ $\sigma t_M + \alpha$

λ Tidal wave length, ft

λ_o Frictionless tidal wave length, ft

μ Frictional wave damping factor, 1/ft

ρ Fluid density, $\text{lb-sec}^2/\text{ft}^4$

σ Tidal frequency, $2\pi/T$

ϕ $2\pi\mu/k$

ONE-DIMENSIONAL ANALYSIS OF SALINITY INTRUSION IN ESTUARIES

PART I: INTRODUCTION

1. The objective of the investigation reported herein is to develop analytical procedures for the determination of the distribution of salinity in an estuary. The intrusion of saline water in the tidal portion of a river involves the basic mechanism of mass transfer by turbulent diffusion and mass transfer by convective currents which are associated with tidal motion and the presence of liquids of different density. Usually the engineer is called upon to predict the change in the salinity distribution in a particular estuary which will occur as a result of a change in estuary geometry or hydraulic characteristics. Common examples of such changes are the dredging of deeper navigation channels and changes in fresh-water flow rates due to upstream diversions or regulation. While such problems have been studied by engineers and oceanographers for many years, in almost all instances the concern has been with a particular estuary. In order to divorce the investigation from a particular geometry and to simplify the problem, the present study is confined to the case of a rectangular estuary of constant mean depth and width.

Previous Investigations

2. An evaluation of the state of knowledge of salinity-intrusion phenomena in estuaries was prepared in 1950 by the Committee on Tidal Hydraulics.[16*] A review of estuarine hydrography has been given by Pritchard[13] in which estuaries are classified in terms of the directions of the advective and nonadvective transport processes. The estuary of this study is of the partially mixed class (type B in reference 13) in which mixing occurs between the fresh water moving down the estuary and the saline water moving up the estuary.

3. Prior to 1950 the analysis of longitudinal salinity distributions

---

* Raised numerals refer to similarly numbered items in the list of references at end of text.

was based on the concept of the tidal prism. The most precise formulation
of the tidal-prism approach is due to Ketchum[11] who suggested dividing an
estuary into segments having lengths equal to the average distance tra-
versed by a particle of water on the flood tide. Within each segment it is
assumed that there is complete mixing at high tide. The method is, there-
fore, only applicable for those estuaries which can be said to approach the
fully mixed condition. Such estuaries are characterized by extremely large
ratios of tidal prism to river discharge.

4. For example, even though the Delaware estuary has a tidal prism
to fresh-water discharge ratio of the order of 100, it still exhibits char-
acteristics of a partially mixed estuary in the sense that salinity trans-
fer by gravitational convection currents is quite strong.

5. Arons and Stommel[1] have proposed a mixing-length theory of tidal
mixing as a means of treating the time average (over a tidal cycle) salin-
ity distribution in a rectangular estuary. The one-dimensional
conservation-of-salt equation was employed with a convective term for the
river flow and a horizontal eddy diffusivity. The latter is assumed to be
equal to the product of the maximum tidal velocity at the estuary entrance,
the tidal excursion length, and a constant of proportionality. By inte-
grating the conservation equations, a family of salinity distribution
curves is obtained in terms of the distance along the estuary divided by
the total length of salinity intrusion. The results are primarily useful
as a classification of estuaries by means of a "flushing number" obtained
by a best fit of field salinity measurements with one of the family of
curves.

6. By contrast, the present report will treat the problem of pre-
dicting the instantaneous salinity distribution, and therefore the intru-
sion lengths, in terms of the tidal and hydraulic properties and certain
boundary conditions to be determined at the ocean entrance to the estuary.
It is therefore necessary to consider the time-dependent conservation-of-
salt equation. It is this approach which will be followed in the present
study.

Experimental and Analytical Program

7. The experimental work was conducted at the Waterways Experiment

Station in a horizontal, rectangular lucite flume 327 ft long and 9 in.
wide. The mean water depth in the flume was 6 in. in the majority of the
tests. One end of the flume is closed and contains provision for the in-
troduction of fresh water at a controlled rate; the opposite end of the
flume is connected to a large tidal basin wherein a constant salinity and
a simple harmonic tide can be maintained. Twenty runs representing various
test conditions were used in the analysis; however, the total number of
flume tests was larger than this because of duplication of certain runs and
incomplete data in some of the earlier tests.

8. A detailed description of the salinity flume and the method of
conducting the tests is contained in reference 17. A summary of the
physical characteristics of the flume tests is given in table 1 in terms of
tidal amplitude and period, salinity in the tidal basin, fresh-water dis-
charge, and flume roughness. The roughness was obtained by use of 1/4-in.-
square lucite strips, spaced on 2-in. centers. For the roughness desig-
nated as "side," the strips were attached to the sidewalls only; the desig-
nation "bottom" indicates that the strips were attached to the bottom only;
and "smooth" indicates the absence of strips.

9. In a rectangular estuary of constant cross section, with a tidal
range sufficient to promote vertical mixing, the longitudinal salinity dis-
tribution may be treated one-dimensionally. In this sense the term salin-
ity s refers to the average concentration of salt at a particular sec-
tion x and instant of time t.

10. Using the notation shown in fig. 1, the one-dimensional salinity
distribution problem can be considered in terms of nine independent vari-
ables. In general,

$$s = f \left(x, \ t, \ L, \ h, \ a, \ T, \ U, \ s_o, \ \text{and roughness} \right)$$
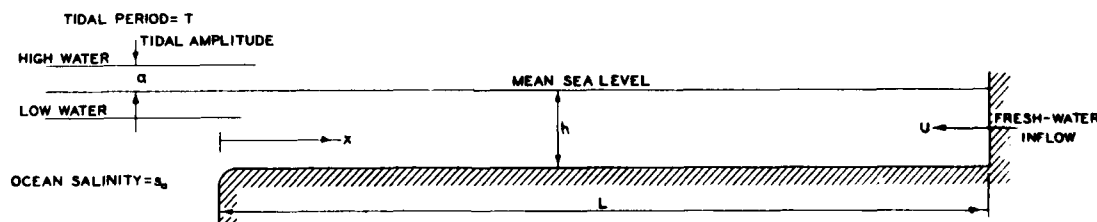
Fig. 1. Notation for one-dimensional salinity intrusion

4

11. The specific objective of this phase of the investigation is the correlation of the experimental data by means of an analytical study of the salinity-intrusion mechanism. Throughout the analysis, the ultimate objective of applying the information gained in the one-dimensional study to actual estuaries is of primary importance. Whenever a choice of analytical procedures is available, the one most applicable to natural conditions is chosen. Approximations, which in certain cases are unnecessary in the one-dimensional problem, are introduced (sometimes at the expense of mathematical rigor) to further achieve this goal.

PART II: THEORETICAL CONSIDERATIONS

12. Salinity intrusion is closely associated with the tidal motion
in an estuary. The tides are the primary source of energy for the turbu-
lent mixing of fresh and salt water; in addition, large convective motions
are associated with the great length of tidal waves. For convenience, the
theoretical considerations will be presented in two sections, the first
dealing only with the tidal dynamics and the second with the intrusion of
salt.

Tidal Dynamics

13. At the mouth of an estuary a cyclical rise and fall of the water
surface exists as the result of tidal action in the ocean. The tidal mo-
tion within the estuary is entirely the result of tide-producing forces at
the mouth and is termed a co-oscillating tide. If friction is neglected,
the co-oscillating tide becomes a standing wave and the extreme water
levels occur simultaneously over the entire basin. A standing wave in an
estuary having a length L less than one-quarter the length of the stand-
ing wave λ is shown in fig. 2.

Fig. 2. Standing wave in a channel where $L < \lambda/4$

In this case the range of tide at the end of the estuary is considerably
greater than that at the ocean entrance. For frictionless tidal waves,
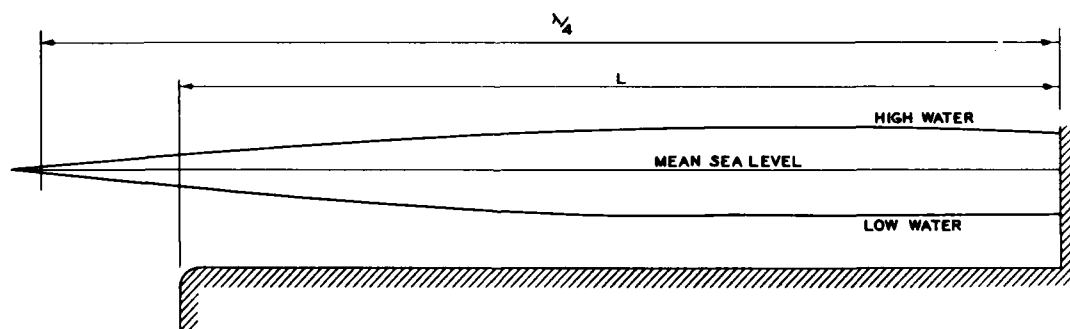$c_o = \sqrt{gh}$ and $T = 12.4$ hr, $\lambda_o = c_o T = \sqrt{gh}\, T$. For an estuary having a
mean depth of 50 ft, the wave length is 325 miles; thus the lengths of many
natural estuaries are less than $\lambda/4$.

14. A study of the U. S. Coast and Geodetic Survey tide tables reveals that few, if any, natural estuaries are accurately represented by a frictionless standing wave. It is generally observed that the time of high water in the landward direction is progressively later with respect to high water at the ocean end. In a uniform estuary this time lag must be entirely attributed to frictional effects. In the damped co-oscillating tide the amplitude of the incoming wave decreases in the landward direction, is reflected at the end of the estuary, and again undergoes damping in its progress toward the ocean. In the limiting case the incoming wave is completely dissipated by friction and the amplitude at the head of the basin and hence that of the reflected wave is zero. In this case the co-oscillating tide reduces to a single progressive wave subject to extreme damping.

15. The basic theory of the co-oscillating tide is based on the classical work of Defant[2] and Fjeldstad.[5] Einstein and Fuchs[4] have used a similar approach to predict tidal amplitudes and velocities in a uniform rectangular estuary, the hydraulic roughness of which is a known constant. Recently Perroud[12] has extended this work to include prismatic channels whose shape can be described by linear or exponential expressions. These investigators have linearized the equation of motion by replacing the quadratic friction term by a constant times the velocity. This is rationalized on the basis that the frictional work done over a tidal cycle is made identical for both the linear and the quadratic damping. However, the problem of the (a priori) choice of the proper numerical value of the friction coefficient for the linear damping term has not been resolved. A necessary additional assumption is that this coefficient must be constant with respect to x . Stepwise procedures for tidal computations have been outlined by Dronkers and Schoenfeld;[3] in all cases bottom frictional coefficients and tidal velocities or elevations must be known boundary conditions.

16. A somewhat different approach based on the assumption of exponential damping of the incident and reflected waves was suggested by Redfield[14] and was also used by the authors[9] in the development of a mathematical model for the tidal dynamics of the Bay of Fundy. The procedure requires that tidal ranges be known at several points within the

estuary. In the case of a rectangular estuary this information permits the calculation of the damping coefficient and the tidal velocities. The primary advantage of the method is that it can be applied to natural estuaries when it is desired to have information on the variation of tidal velocities along the axis of the estuary for use in salinity-intrusion studies. In these cases the so-called "damping factor" includes both the effect of cross-sectional area changes and frictional resistance. The annual tide tables of the Coast and Geodetic Survey provide sufficiently detailed information on tidal ranges in estuaries for the approximate calculation of local velocities. While measurements of tidal velocities in the Bay of Fundy are scanty, the available data seem to confirm the predicted values.

17. Both the method outlined above and the method of Einstein and Fuchs can be applied, with equal facility and mathematical rigor, to the uniform rectangular estuary. The Einstein-Fuchs theory was successfully compared with the Waterways Experiment Station data in the preliminary report by the authors in June 1957. In the present report the formulation described in the preceding paragraph will be used in view of its immediate applicability in the case of natural estuaries.

Co-oscillating Tide with Exponential Damping

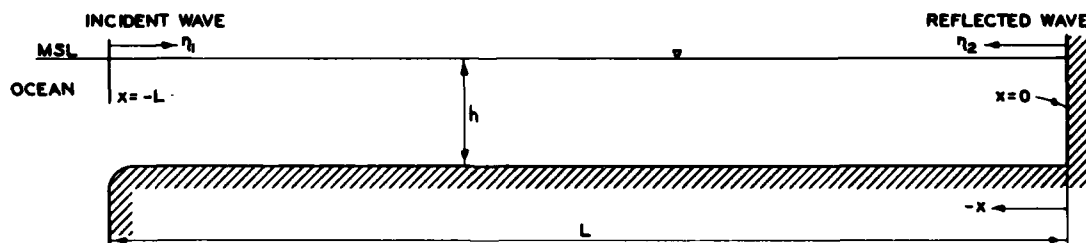18. Fig. 3 is a definition sketch showing the notation to be used in the tidal analysis.

Fig. 3. Definition sketch for a damped co-oscillating tide in a uniform channel

Tidal elevations

19. The tide in the channel is assumed to be composed of two waves traveling in opposite directions: (a) an incident wave entering from the

8

ocean (traveling in the positive x direction) and having a surface eleva-
tion η_1 which is a function of x and t (time); and (b) a reflected
wave (traveling in the negative x direction) having a surface elevation
η_2, also a function of x and t. If it is assumed that the amount of
energy dissipated is proportional to the total energy of the wave, the in-
troduction of friction leads to an exponential decrease of the amplitude.
The surface elevations of the incident and reflected waves, respectively,
are then given by the following equations:

$$\eta_1 = A_o\, e^{-\mu x}\, \cos\,(\sigma t - kx) \qquad (1)$$

$$\eta_2 = A_o\, e^{\mu x}\, \cos\,(\sigma t + kx) \qquad (2)$$

where

$\sigma = 2\pi/T$ (T = period of ocean tide)

$k = 2\pi/\lambda$ (λ = wave length)

A_o = amplitude of wave at end of channel ($x = 0$)

μ = damping coefficient

$t = 0$ (corresponds to high water at end of channel)

$e = 2.718$

20. The tidal elevation η (above or below msl) at any time t and
place x in the channel is given by the sum of the amplitudes of the in-
cident and reflected waves; thus

$$\eta = \eta_1 + \eta_2 = A_o\,[e^{-\mu x}\, \cos\,(\sigma t - kx) + e^{\mu x}\, \cos\,(\sigma t + kx)] \qquad (3)$$

The time of high water at any position in the estuary occurs when
$\partial\eta/\partial t = 0$; therefore

$$\frac{\partial \eta}{\partial t} = e^{-\mu x}\, \sin\,(\sigma t - kx) + e^{\mu x}\, \sin\,(\sigma t + kx) = 0 \qquad (4)$$

Equation 4 may be expanded and regrouped in the following form:

$$(e^{\mu x} + e^{-\mu x})\, \sin\,\sigma t\, \cos\,kx + (e^{\mu x} - e^{-\mu x})\, \cos\,\sigma t\, \sin\,kx = 0$$

and since $\dfrac{e^{\mu x} - e^{-\mu x}}{e^{\mu x} + e^{-\mu x}} = \tanh \mu x$,

$$\tan \sigma t_H = -\tan kx \tanh \mu x \qquad (5)$$

21. σt_H is the relative time of high water at any position in the estuary with respect to the time of high water at the end of the channel ($\sigma t_H = 0$). From equation 5 the value of σt_H , in degrees, is given by

$$\sigma t_H = \tan^{-1} (-\tan kx \tanh \mu x) \qquad (6)$$

In order to determine the damping coefficient μ from the experimental tidal elevation, it is convenient to express the local high-water tidal amplitude η_H in terms of the high-water amplitude at the end of the channel η_{oH} . The local high-water amplitude at any point along the channel can be obtained by substituting the time angle for high water (σt_H) from equation 6 into equation 3, whence

$$\eta_H = 2A_o \sqrt{\tfrac{1}{2}(\cos 2kx + \cosh 2\mu x)} \qquad (7)$$

At the end of the estuary ($x = 0$), $\cos (0) = \cosh (0) = 1$; therefore, $\eta_{oH} = 2A_o$ and the desired ratio of local high water to high water at the landward end is

$$\frac{\eta_H}{\eta_{oH}} = \sqrt{\tfrac{1}{2}(\cos 2kx + \cosh 2\mu x)} \qquad (8)$$

At the ocean entrance ($x = -L$), $\eta_H = a$ is the amplitude of the ocean tide; hence

$$\frac{a}{\eta_{oH}} = \frac{a}{2A_o} = \sqrt{\tfrac{1}{2}(\cos 2kL + \cosh 2\mu L)} \qquad (9)$$

In a channel of uniform cross section and roughness, both k and μ would be expected to be constants. This may be stated algebraically as

$$\mu = \left(\frac{\phi}{2\pi}\right) k \qquad (10)$$

10

and equations 6 and 8 may be rewritten as follows:

$$\sigma t_H = \tan^{-1}\left[-\tan kx \ \tanh\left(\frac{\emptyset kx}{2\pi}\right)\right] \tag{11}$$

$$\frac{\eta_H}{\eta_{oH}} = \sqrt{\frac{1}{2}\left[\cos 2kx + \cosh\left(\frac{\emptyset kx}{2\pi}\right)\right]} \tag{12}$$

A plot of the tidal amplitude ratio η_H/η_{oH} versus the time angle of high water σt_H may therefore be made with the independent variables $\emptyset$ and kx defining a family of curves. Thus, if the tidal amplitude and time of high water are known at several points along the channel, these values when plotted in the manner suggested above should fall along a curve of $\emptyset$ = constant. In principle, both μ and k could be determined by knowing the time and amplitude of the tide at the closed end of the channel and at only one other intermediate section. In practice, the graphical method described above gives values of μ and k which are the best fit for all of the available data.

Tidal velocities

22. The equation for the tidal velocity can be derived by making use of the continuity equation for unsteady, nonuniform motion.

23. The continuity equation for the incident wave (considering amplitudes to be small compared to depth) is given by:

$$\frac{\partial u_1}{\partial x} = -\frac{1}{h}\frac{\partial \eta_1}{\partial t} \tag{13}$$

where u_1 is the velocity due to the incident wave of amplitude η_1. With η_1 given by equation 1,

$$\frac{\partial \eta_1}{\partial t} = -A_o \ e^{-\mu x} \ \sigma \ \sin(\sigma t - kx)$$

and the continuity equation 13 becomes:

$$\frac{\partial u_1}{\partial x} = \frac{A_o \ \sigma}{h} \ e^{-\mu x} \ \sin(\sigma t - kx) \tag{14}$$

u_1 is obtained by integrating with respect to x ,

$$u_1 = \frac{A_o \, \sigma}{h} \int e^{-\mu x} \sin (\sigma t - kx) \, dx$$

and by expanding the quantity in parentheses,

$$u_1 = \frac{A_o \, \sigma}{h} \left(\sin \sigma t \int e^{-\mu x} \cos kx \, dx - \cos \sigma t \int e^{-\mu x} \sin kx \, dx \right)$$

or

$$u_1 = \frac{A_o \, \sigma}{h} \left[\sin \sigma t \; e^{-\mu x} \left(\frac{-\mu \cos kx + k \sin kx}{\mu^2 + k^2} \right) \right.$$
$$\left. - \cos \sigma t \; e^{-\mu x} \left(\frac{-\mu \sin kx - k \cos kx}{\mu^2 + k^2} \right) \right] + F(t) \quad (15)$$

The integration constant $F(t)$ may be evaluated by introducing the boundary condition that $u_1 = 0$ at $x = 0$ (end of basin) for all values of time; hence, $F(t) = 0$.

24. Equation 15 may be considerably simplified by the following operations:

$$u_1 = \frac{A_o \, \sigma}{h} \frac{e^{-\mu x}}{\mu^2 + k^2} \left[\sin \sigma t \, (-\mu \cos kx + k \sin kx) \right.$$
$$\left. - \cos \sigma t \, (-\mu \sin kx - k \cos kx) \right]$$

$$u_1 = \frac{A_o \, \sigma}{h} \frac{e^{-\mu x}}{\mu^2 + k^2} \left[k \, (\sin kx \sin \sigma t + \cos kx \cos \sigma t) \right.$$
$$\left. + \mu \, (\sin kx \cos \sigma t - \cos kx \sin \sigma t) \right]$$

$$u_1 = \frac{A_o \, \sigma}{h} \frac{e^{-\mu x}}{\mu^2 + k^2} \left[k \cos (\sigma t - kx) + \mu \sin (kx - \sigma t) \right]$$

$$u_1 = \frac{A_o \, \sigma}{h} \frac{e^{-\mu x}}{\sqrt{\mu^2 + k^2}} \left[\frac{k \cos (\sigma t - kx)}{\sqrt{\mu^2 + k^2}} + \frac{\mu \sin (kx - \sigma t)}{\sqrt{\mu^2 + k^2}} \right] \qquad (16)$$

Let $\cos \alpha = \dfrac{k}{\sqrt{\mu^2 + k^2}}$ and $\sin \alpha = \dfrac{\mu}{\sqrt{\mu^2 + k^2}}$

Then $\tan \alpha = \dfrac{\sin \alpha}{\cos \alpha} = \dfrac{\mu}{k}$ and therefore $\alpha = \tan^{-1} \dfrac{\mu}{k}$.

12

From equation 10, it follows that

$$\alpha = \tan^{-1}\left(\frac{\phi}{2\pi}\right) \tag{17}$$

Returning again to equation 16,

$$u_1 = \frac{A_o \sigma}{h} \frac{e^{-\mu x}}{\sqrt{\mu^2 + k^2}} \left[\cos \alpha \cos (\sigma t - kx) + \sin \alpha \sin (kx - \sigma t)\right]$$

$$u_1 = \frac{A_o \sigma}{h} \frac{e^{-\mu x}}{\sqrt{\mu^2 + k^2}} \left[\cos (kx - \sigma t - \alpha)\right]$$

However, since the cosine is an even function,

$$u_1 = \frac{A_o \sigma}{h} \frac{e^{-\mu x}}{\sqrt{\mu^2 + k^2}} \left[\cos (\sigma t - kx + \alpha)\right] \tag{18}$$

25. By a similar procedure the continuity equation is written for the reflected wave, with the result:

$$u_2 = - \frac{A_o \sigma}{h} \frac{e^{\mu x}}{\sqrt{\mu^2 + k^2}} \left[\cos (\sigma t + kx + \alpha)\right] \tag{19}$$

26. The tidal velocity at any time and position along the channel is given by the sum of u_1 and u_2; thus,

$$u = \frac{A_o \sigma}{h} \frac{1}{\sqrt{\mu^2 + k^2}} \left[e^{-\mu x} \cos (\sigma t - kx + \alpha) - e^{\mu x} \cos (\sigma t + kx + \alpha)\right] \tag{20}$$

Since $A_o = \eta_{oH}/2$ and η_{oH} may be eliminated by means of equation 9, the above equation may be rewritten as

$$u = \frac{a\sigma}{kh} \frac{e^{-\mu x} \cos (\sigma t - kx + \alpha) - e^{\mu x} \cos (\sigma t + kx + \alpha)}{\sqrt{2 \left[\left(\frac{\mu}{k}\right)^2 + 1\right] (\cos 2kL + \cosh 2\mu L)}} \tag{21}$$

The maximum velocity at the ocean end of the channel will be of interest in the salinity analysis; the maximum velocity at any position occurs when $\partial u/\partial t = 0$; therefore, from equation 21:

$$\sigma t_M = \tan^{-1} (-\tan kx \coth \mu x) - \alpha \qquad (22)$$

This value of σt_M, when substituted into equation 21, will give the maximum velocity at any position x. By putting $x = -L$ in equations 21 and 22, the maximum velocity at the ocean entrance can be calculated.

Tidal energy dissipation

27. One of the important concepts in turbulent-diffusion theory is the relation between the diffusion coefficient, the rate of energy dissipation per unit mass of fluid, and the scale of turbulence. In a partially or well-mixed estuary, the primary source of mixing energy is the tidal motion. The rate of energy dissipation per unit mass due to the tidal motion should therefore be a useful factor in the correlation of the salinity intrusion with the tidal characteristics of the channel.

28. For waves of small steepness, the energy of a progressive oscillatory wave per unit of surface area is

$$E = \frac{\gamma \, a_x^2}{2}$$

where a_x is the local maximum amplitude of the wave. The flux of energy P across a vertical section is given by

$$P = Ecb \; (\frac{ft\text{-}lb}{sec})$$

where c is the wave celerity and b the channel width.

29. In the damped co-oscillating tidal analysis, the tidal motion is determined by the superposition of two waves, one (the incident wave) proceeding from the ocean entrance to the closed end of the estuary and the other (the reflected wave) from the closed end to the entrance. Thus, the energy flux for the incident wave (moving in the $+x$ direction) of amplitude $A_o \, e^{-\mu x}$ (see equation 1) is

$$P_1 = \frac{cb\gamma}{2} A_o^2 \, e^{-\mu x} \; ,$$

and that for the reflected wave (moving in the $-x$ direction) is

14

$$P_2 = -\frac{cb\gamma}{2} A_o^2 e^{2\mu x}$$

The total energy flux at an intermediate section is therefore

$$P = -\frac{cb\gamma}{2} A_o^2 (e^{2\mu x} - e^{-2\mu x})$$

or

$$P = -cb\gamma A_o^2 \sinh 2\mu x \tag{23}$$

(Here it is seen that if $\mu = 0$ (standing wave) the total energy flux $P = 0$.)

30. The energy flux at the ocean entrance $(x = -L)$ is therefore

$$P_L = cb\gamma A_o^2 \sinh 2\mu L$$

The change in the energy flux between the ocean entrance and any intermediate section is equal to the rate of energy dissipation in that portion of the channel; hence,

$$\text{Rate of energy dissipation} = P_L - P = cb\gamma A_o^2 (\sinh 2\mu L + \sinh 2\mu x)$$

The mass of fluid in this same portion of the channel is $\rho bh (L + x)$ and the rate of energy dissipation per unit mass G_x is given by

$$G_x = \frac{gc}{h} A_o^2 \left(\frac{\sinh 2\mu L + \sinh 2\mu x}{L + x} \right) \tag{24}$$

The rate of energy dissipation per unit mass for the entire channel is given by setting $x = 0$; hence,

$$G = \frac{gc}{hL} A_o^2 \sinh 2\mu L \tag{25}$$

The ratio

$$\frac{G_x}{G} = \frac{1 + \dfrac{\sinh 2\mu x}{\sinh 2\mu L}}{1 + \dfrac{x}{L}}$$

and the maximum value of this ratio occurs at the ocean entrance where

$x \rightarrow -L$, in the limit the ratio $\dfrac{G_L}{G} = \dfrac{2\mu L}{\tanh 2\mu L}$. If the argument of the

hyperbolic function ($2\mu L$) is small, the maximum value of G_x/G will not differ appreciably from unity; hence, it is generally sufficient to use the total energy dissipation rate as given by equation 25 as representative of the entire channel. The factor A_o can be eliminated by means of equation 9, and equation 25 thus becomes

$$G = \frac{gc\ a^2}{2hL} \left(\frac{\sinh 2\mu L}{\cos 2kL + \cosh 2\mu L} \right) \tag{26}$$

Note that in the above equation the wave celerity $c = \lambda/T = \sigma/k$. In general, due to the effect of friction, the celerity will be less than $\sqrt{gh}$ as in the frictionless case.

Summary

31. For convenient reference in the later sections, the important equations for the tidal dynamics are summarized below.

32. The two independent parameters describing the tidal motion are the wave length expressed by $k = 2\pi/\lambda$ and the damping modulus μ . If the amplitude and time of high water at the closed end and at various stations along the channel are known, μ and k can be determined from the following two equations:

$$\sigma t_H = \tan^{-1} (-\tan kx \tanh \mu x) \tag{6}$$

$$(\sigma t_H = 0 \text{ at closed end})$$

$$\frac{\eta_H}{\eta_{oH}} = \sqrt{\frac{1}{2}(\cos 2kx + \cosh 2\mu x)} \tag{8}$$

$$(\eta_{oH} = \text{elevation of high water} \atop \text{at closed end})$$

The maximum tidal velocity at the ocean entrance of the channel u_o is given by equation 21 with $x = -L$,

$$u_0 = \frac{a\sigma}{kh} \frac{e^{\mu L} \cos(\theta + kL) - e^{-\mu L} \cos(\theta - kL)}{\sqrt{2\left[\left(\frac{\mu}{k}\right)^2 + 1\right](\cos 2kL + \cosh 2\mu L)}} \qquad (21a)$$

where

$$\theta = \sigma t_M + \alpha = \tan^{-1}(-\tan kL \coth \mu L) \qquad (22a)$$

The rate of energy dissipation per unit mass of fluid due to tidal friction is given by:

$$G = \frac{g\sigma a^2}{2khL}\left(\frac{\sinh 2\mu L}{\cos 2kL + \cosh 2\mu L}\right) \qquad (26)$$

Salinity Intrusion

33. The basic relation in the salinity-intrusion analysis is the equation for the conservation of the mass of salt, otherwise known as the convective-diffusion equation. For a turbulent, incompressible fluid this equation has the following general form (see reference 15, page 159):

$$\frac{\partial s}{\partial t} + u\frac{\partial s}{\partial x} + v\frac{\partial s}{\partial y} + w\frac{\partial s}{\partial z} = \frac{\partial}{\partial x}\left(D_x \frac{\partial s}{\partial x}\right) + \frac{\partial}{\partial y}\left(D_y \frac{\partial s}{\partial y}\right) + \frac{\partial}{\partial z}\left(D_z \frac{\partial s}{\partial z}\right) \qquad (27)$$

where u, v, w are the x, y, z components of the fluid velocity and D_x, D_y, D_z are turbulent diffusion coefficients (ft^2/sec).

34. The above equation expresses the condition that the net mass transfer of salt by convection and diffusion into an elemental volume is equal to the time rate of accumulation of material in that volume.

35. In the one-dimensional analysis, the salinity gradients in the y and z directions are neglected and equation 27 becomes

$$\frac{\partial s}{\partial t} + u\frac{\partial s}{\partial x} = \frac{\partial}{\partial x}\left(D_x \frac{\partial s}{\partial x}\right) \qquad (28)$$

36. At any point in the channel, the x component of the fluid velocity is equal to the sum of the velocity due to tidal motion $u(x,t)$ and the fresh-water velocity $-U$; hence,

$$\frac{\partial s}{\partial t} + u(x,t)\,\frac{\partial s}{\partial x} - U\,\frac{\partial s}{\partial x} = \frac{\partial}{\partial x}\left(D_x\,\frac{\partial s}{\partial x}\right) \tag{29}$$

37. In the salinity-intrusion analysis it will be convenient to take $x = 0$ at the ocean entrance of the estuary (see fig. 1); in addition, time $t = 0$ will refer to low tide in the ocean. The difficulties associated with finding a general solution for equation 29 are overcome by treating the problem in two distinct parts.

Salinity distribution at
low tide (quasi-steady state)

38. It is recognized that although the salinity concentration depends on time, it varies in a periodic manner due to the tide. Equation 29 may therefore be considerably simplified by considering only average values where the averaging is over a period of time of the order of a tidal cycle. Since the tidal velocity $u(x,t)$ is harmonic, its average value over a cycle is zero and the quasi-steady-state conservation equation may be stated as

$$-U\,\frac{\partial \bar{s}}{\partial x} = \frac{\partial}{\partial x}\left(D_x\,\frac{\partial \bar{s}}{\partial x}\right) \tag{30}$$

39. The basic assumption that the quasi-steady-state salinity distribution can be represented by the one-dimensional convective-diffusion equation 30 warrants further consideration. This equation represents an equilibrium between the seaward mass transfer by the average fresh-water velocity U and the landward mass transfer due to turbulent diffusion. However, in the estuary intrusion problem there is an additional mechanism for the transport of salt in the landward direction. This process, which will be called gravitational convection, is caused by the difference in specific weight of the ocean and fresh water. The saline wedge, which occurs in estuaries entering an ocean with a negligible tidal range, is an extreme example of the upstream penetration of salt by gravitational convection. In the treatment of the wedge problem it is possible to neglect the effect of the turbulent diffusion. However, even in the so-called well-mixed estuary, it is by no means obvious that the effect of gravitational convection may be neglected. The gravitational convection of salt depends on the vertical density gradients which cannot be represented in

the one-dimensional equation 30. The only possible basis for a continuation of the one-dimensional approach in the light of this difficulty is the assumption that the diffusion coefficient can reflect both eddy diffusion and gravitational convection. This assumption has been verified by a series of experiments conducted under the authors' supervision at the Massachusetts Institute of Technology Hydrodynamics Laboratory (see references 6 and 10).

40. The MIT tests were carried out in a rectangular channel in which homogeneous turbulence was generated by the vertical oscillation of metal screens immersed in the fluid. The test program included unsteady- and steady-state diffusion and convection of fluids of different densities for various intensities of fluid turbulence. It was found that longitudinal salinity distributions could be described by the one-dimensional conservation-of-mass equation in which the turbulent diffusion coefficient D_x was replaced by a larger apparent diffusion coefficient D_x' . In other words,

$$D_x' = D_x + \Delta D_x \qquad (31)$$

where D_x is the eddy diffusivity and ΔD_x is a mass-transfer coefficient due to gravitational convection. These observations are not unreasonable if it is considered that the gravitational convection gives rise to large-scale internal circulations which may be thought of as eddies. In this sense ΔD_x is also a turbulent diffusion coefficient due to eddies having mixing lengths many orders of magnitude larger than the normal eddy scale of the shear-generated turbulence. The apparent diffusion coefficient D_x' should therefore replace the turbulent coefficient D_x in the equations developed in paragraphs 33-36. Equation 30 may now be integrated with respect to x , noting that the fresh-water velocity U is constant in a uniform rectangular estuary.

$$U\bar{s} = -D_x' \frac{\partial \bar{s}}{\partial x} + F(t) \qquad (32)$$

where $F(t)$ is the integration constant for the partial differential equation. $F(t)$ is arbitrarily set equal to zero since it can be shown that any other value has the effect of introducing a constant displacement

of the salinity in the x direction. In so doing it is assumed that the salinity distribution given by equation 32 represents conditions at successive times of <u>low tide</u> in the estuary, since at this time the salinity extends a minimum distance into the estuary; hence,

$$\bar{Us} = -D'_x \frac{d\bar{s}}{dx} \tag{33}$$

Separating the variables and integrating again,

$$\int \frac{d\bar{s}}{\bar{s}} = -U \int \frac{dx}{D'_x} \quad \text{or} \quad \ln\bar{s} + C_1 = -U \int \frac{dx}{D'_x} \tag{34}$$

In order to complete equation 34 it is necessary to specify the manner in which D'_x varies with x . Further consideration of this point will be given following the discussion of the second part of the solution of the salt-transfer equation 29.

Salinity convection
<u>within a tidal cycle</u>

41. If it is accepted that the salinity distribution is known at low tide (from the above analysis), the remainder of the one-dimensional salinity-intrusion problem consists of determining the salinity distribution at other instants of time within the tidal cycle.

42. A physical appreciation of the reasoning involved may be gained by imagining the channel to have a vertical barrier separating regions of fresh and salt water just prior to the start of a test. As the barrier is removed the tide generator at the ocean end is started and fresh water is introduced at the closed end of the estuary. During the <u>first few tidal cycles</u> a large amount of diffusion between fresh and salt water must take place within each cycle. It is not difficult to imagine that the amount of diffusion taking place during each tidal cycle will progressively diminish and that after a large number of cycles (under constant tidal and fresh-water inflow conditions) the diffusion during one cycle will be small. It is therefore postulated that an equilibrium condition or a quasi-steady state has been reached in which the salinity distribution does not change appreciably in a tidal cycle due to longitudinal diffusion. The principal change in salinity at a fixed point is therefore a result of

the tidal velocity carrying the salinity up and down the estuary. The diffusion process due to fresh-water inflow and the tidal velocities are very important in determining the form of the salinity distribution but during one tidal cycle their effects are considered negligible. Qualitatively, this is equivalent to setting the right-hand side of equation 29 equal to zero. Therefore, if the low-tide salinity distribution is known, the salinity distribution at any other time in the tidal cycle may be found by solving the convection equation:

$$\frac{\partial s}{\partial t} + [u(x,t) - U] \frac{\partial s}{\partial x} = 0 \tag{35}$$

In partially and well-mixed estuaries the tidal velocities $u(x,t)$ are generally large compared to the fresh-water velocity U; hence equation 35 may be represented by

$$\frac{\partial s}{\partial t} + u(x,t) \frac{\partial s}{\partial x} = 0 \tag{36}$$

The general solution of this form of partial differential equation (reference 8, page 371) is of the form

$$X_2 = f(X_1)$$

where $X_1(s,x,t) = C_1$ and $X_2(s,x,t) = C_2$ are any two independent solutions of

$$dt = \frac{dx}{u(x,t)} = \frac{ds}{0} \tag{37}$$

One solution is $ds = 0$ and hence $C_1 = s$; the second solution can only be obtained readily if the variables in the expression for the tidal velocity $u(x,t)$ are separable. At this point it would be desirable to introduce the general expression for the tidal velocity, equation 21, previously developed. However, the x and t variables are clearly not separable in this equation, and it is necessary to find a suitable approximation for $u(x,t)$ which is valid at least over the region of

salinity intrusion in the channel. For this purpose the continuity equation 13 is written for the tidal velocity.

$$\frac{\partial u}{\partial x} = -\frac{1}{h}\frac{\partial \eta}{\partial t} \tag{38}$$

If it is assumed that the water surface in the estuary oscillates horizontally, $\eta = -a \cos \sigma t$ ($t = 0$ at low tide). Then $\frac{\partial u}{\partial x} = -\frac{a\sigma}{h} \sin \sigma t$.

Upon integrating, $u(x,t) = -\frac{a\sigma x}{h} \sin \sigma t + F(t)$. Since in this simple case the velocities are 90 degrees out of phase with the elevations, the following boundary condition may be used to determine $F(t)$: $u = u_0 \sin \sigma t$ at $x = 0$ (ocean entrance). Therefore

$$u(x,t) = u_0 (1 - \delta x) \sin \sigma t \tag{39}$$

where $\delta = \dfrac{a\sigma}{hu_0}$

This development leads to a linear decrease of the tidal velocity in the landward direction in which the x and t variables in the equation are separable. The point to stress is that in this process the maximum velocity at the ocean entrance of the channel is not specified and the correct value computed on the basis of the damped co-oscillating tide may therefore be used (equation 21a). A numerical comparison of equations 39 and 21a given in a later section shows that the linear approximation does not lead to serious errors. Thus it is possible to approximate surface elevations and velocity variations by linear laws for damped tides.

43. The second solution of equation 37

$$dt = \frac{dx}{u(x,t)}$$

is readily obtained by substitution of equation 39; therefore,

$$u_0 \int \sin \sigma t \, dt = \int \frac{dx}{(1 - \delta x)}$$

and

$$C_2 = (1 - \delta x) \, e^{-(a/h) \cos \sigma t}$$

Therefore the general solution of the salinity-convection equation 36 is given by the following:

$$C_1 = f(C_2)$$

or

$$\frac{s}{s_0} = f\left[(1 - \delta x)\, e^{-(a/h)} \cos \sigma t\right] \qquad (40)$$

If the salinity distribution is known at $t = 0$, low tide, the salinity distribution at any other instant of time can be determined from equation 39.

Variation of the diffusion coefficient along the channel

44. A solution of the quasi-steady-state salinity distribution, equation 34, depends upon the assumed variation of the apparent diffusion coefficient with x.

> a. The simplest assumption is that $D_x' = \text{constant} = D'$.
> Hence, equation 34 becomes

$$\ln \bar{s} + C_1 = -\frac{Ux}{D'} \qquad (41)$$

> The boundary condition for the evaluation of C_1 must express the fact that the salinity is known at some x; however, the only fixed salinity is that in the ocean. It is physically obvious that during the low-tide cycle the salinity at the ocean entrance of the channel ($x = 0$) cannot be that of the ocean itself due to the dilution effect of the fresh-water flow. To circumvent this difficulty a model is postulated in which the channel is extended seaward an imaginary distance B to a point where the ocean salinity s is maintained constant at all times. Hence, $\bar{s} = s_0$ at $x = -B$, and equation 41 becomes

$$\frac{\bar{s}}{s_0} = e^{-\frac{U}{D'}(x + B)} \qquad (42)$$

> which expresses the low-tide salinity distribution as a simple exponential curve.

> b. A second and more realistic assumption regarding the apparent diffusion coefficient ($D_x' = D_x + \Delta D_x$) is that it

decreases in the landward direction. The reasons for the decrease are twofold:

(1) The eddy diffusivity D_x would be expected to decrease in the landward direction due to the decrease in the magnitude of the tidal velocities.

(2) Experiments in the MIT diffusion flume[7] have shown that ΔD_x is proportional to the local density difference along the estuary. Since $\Delta\rho/\rho$ decreases as x increases (in the landward direction), ΔD_x is inversely proportional to x.

The simplest assumption compatible with the above is that D_x' is an inverse function of x having the form

$$D_x' = \frac{C}{x + B} = \frac{D_o' B}{x + B} \tag{43}$$

Therefore at $x = 0$

$$D_x' = D_o'$$

while at $x = -B$

$$D_x' = \infty$$

and for large x

$$D_x' \longrightarrow 0$$

The fact that D_x' approaches an infinite value at $x = -B$ is consistent with the fact that if the walls of the channel are imagined to extend to $x = -B$ an infinite amount of mixing would be required to maintain constant salinity throughout the tidal cycle.

45. Equation 34 can be written as

$$\ln\bar{s} + C_2 = -\frac{U}{D_o' B} \int (x + B)\, dx = -\frac{U(x + B)^2}{2D_o' B} \tag{44}$$

and using the same boundary condition $\bar{s} = s_o$ at $x = -B$, equation 44 becomes

$$\frac{\bar{s}}{s_o} = e^{-W(x + B)^2} \tag{45}$$

where

$$W = \frac{U}{2D_o' B}$$

Equation 45 has the form of a Gaussian or normal error curve. Fig. 4 shows schematically the boundary condition and the characteristic shape of the low-water salinity distribution curves for the two cases derived above.
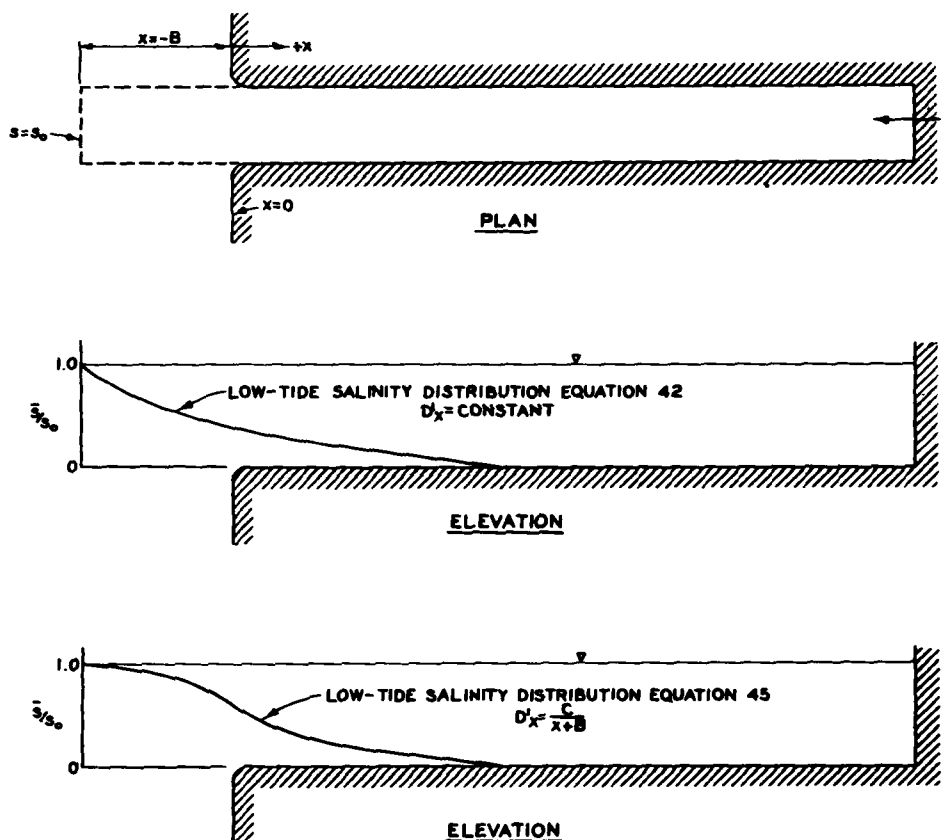

Fig. 4. Schematic salinity distribution at low tide

The experimental results presented later in this report indicate that the assumption of D_x' as an inverse function of x is valid, and the remainder of the analytical development is therefore based on this assumption.

Instantaneous salinity distributions

46. The preceding developments may be summarized as follows: Equation 45 describes the salinity distribution at low tide $(t = 0)$

$$\frac{\bar{s}}{s_o} = e^{-W(x_L + B)^2} \quad \text{for} \quad (x_L + B) > 0 \tag{45}$$

As a reminder that when x is varied in equation 45 it produces the

salinity distribution at low tide only, the subscript L is added to the x in this equation.

47. The salinity distribution at any other instant of time is given by equation 40

$$\frac{s}{s_o} = f\left[(1 - \delta x)\ e^{-(a/h)\ \cos\ \sigma t}\right] \tag{40}$$

These equations (40 and 45) may be combined to produce an analytical expression for the instantaneous salinity distribution.

48. Assume that it is desired to find the distribution of salinity at time t ; equation 40 implies that salinity at a particular x and t will be equal to the salinity at low tide (x_L and t = 0). The relation between x_L , x , and t can be found as follows:

$$f\left[(\text{equation 40})\right]_{x_L}^{t=0} = f\left[(\text{equation 40})\right]_x^t$$

hence,

$$(1 - \delta x_L)\ e^{-(a/h)} = (1 - \delta x)\ e^{-(a/h)\ \cos\ \sigma t}$$

Solving for x_L :

$$x_L = \frac{1}{\delta} - \frac{(1 - \delta x)}{\delta}\ e^{(a/h)(1 - \cos\ \sigma t)} \tag{46}$$

Upon substitution of x_L into equation 45 the instantaneous salinity distribution equation is obtained:

$$\frac{s(x,t)}{s_o} = \exp\left\{-\frac{U}{2D_o'\ B\ \delta^2}\ \left[1 - (1 - \delta x)\ e^{(a/h)(1 - \cos\ \sigma t)} + \delta B\right]^2\right\} \tag{47}$$

The specification that $x_L + B > 0$ in equation 45 requires that

$$\left[1 - (1 - \delta x)\ e^{(a/h)(1 - \cos\ \sigma t)} + \delta B\right] > 0$$

in equation 47. If the term in brackets is less than zero, the ratio $s(x,t)/s_o$ is to be taken as unity.

49. The maximum intrusion of salinity occurs at high tide when $\sigma t = \frac{2\pi t}{T} = \pi$. For this condition, equation 47 becomes

$$\frac{s_{HW}}{s_o} = \exp \left\{ - \frac{U}{2D_o' B \delta^2} [1 - (1 - \delta x) e^{2a/h} + \delta B]^2 \right\} \qquad (48)$$

Again, $s_{HW}/s_o = 1$ if $[1 - (1 - \delta x) e^{2a/h} + \delta B] < 0$. The _maximum_ or total intrusion length L_t is arbitrarily defined as the point on the high-tide salinity curve at which the salinity is 1/100 of the ocean salinity. Hence, $x = L_t$ when $s_{HW}/s_o = 0.01$, and since $e^{-4.6} = 0.01$,

$$\frac{U}{2D_o' B \delta^2} [1 - (1 - \delta L_t) e^{2a/h} + \delta B]^2 = 4.6$$

Solving for L_t with $\delta = a\sigma/hu_o$

$$L_t = \frac{hu_o}{a\sigma} (1 - e^{-2a/h}) + e^{-2a/h} B \left(3\sqrt{\frac{D_o'}{UB}} - 1 \right) \qquad (49)$$

The first term in equation 49 represents the convective intrusion of salinity due to the tidal excursion, while the second term represents that part of the salinity intrusion due to the diffusion and gravitational convection processes.

50. Following a similar approach, the minimum intrusion length L_m is obtained directly from equation 45 for the condition $\frac{\overline{s}}{s_o} = 0.01$.

$$L_m = B \left(3\sqrt{\frac{D_o'}{UB}} - 1 \right) \qquad (50)$$

Hence, the maximum intrusion length can also be written as

$$L_t = \frac{hu_o}{a\sigma} (1 - e^{-2a/h}) + e^{-2a/h} L_m \qquad (51)$$

The instantaneous salinity distributions and the intrusion lengths can therefore be determined if the quantities D_o' and B are known. The following sections show how they are determined from the experimental data and how they are correlated with the independent quantities governing the tidal and fresh-water motions.

PART III: ANALYSIS OF EXPERIMENTAL RESULTS

51.   The analysis of the experimental results is presented in two sections. The first deals with the determination of the tidal parameters μ (damping modulus) and $k = 2\pi/\text{wave length}$, and the determination of the maximum entrance velocity u_o. The second section treats the determination of the apparent diffusion coefficient D_o' and the boundary condition distance B. A general summary of the physical characteristics of all of the experimental tests is presented in table 1.

Determination of Tidal Parameters μ, k, and u_o

52.   Tests 28, 29, and 30 were run specifically to obtain tidal data on surface elevations and velocities in the WES flume without the effect of salinity variations or fresh-water velocity. The tidal parameters μ and k determined from these tests may then be compared with similar values obtained for other tests to determine the effect of varying amounts of fresh-water discharge, ocean salinity, and flume roughness.

53.   The objectives of the tidal analysis are:

Fig. 5. Variation of amplitude and time of high water along channel

    a. To determine μ and k from the experimental data on water-surface elevations.

    b. To use these values to calculate the maximum velocity u_o at the flume entrance for use in the salinity convection and intrusion equations.

    c. To determine the rate of energy dissipation in the channel for use as a correlating parameter.

54.   As an example of the calculation procedure, the analysis for test 29 will be presented in detail. Fig. 5 is a plot of surface elevation η (above
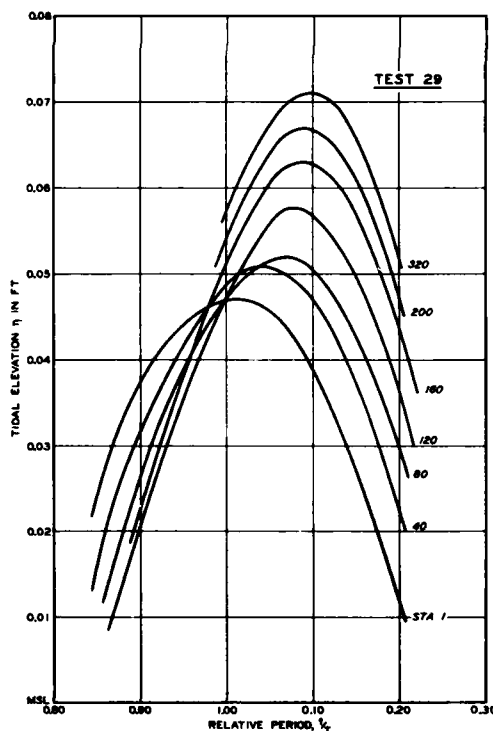
msl) versus time for each station recorded. By graphical interpolation
the amplitudes and times of both high water and low water are recorded for
each station, see columns (2) and (5) in table 2. The averages of the
elevations of both high and low water are listed in column (3), since the
theory assumes a symmetrical tidal wave. The ratio of the average local
amplitude to the amplitude at the closed end η_H/η_{oH} is then computed as
shown in column (4). A similar averaging of the time of high and low
water is given in column (6). Finally the time of high water referred to
zero at the closed end is shown in columns (7) and (8). The values tabu-
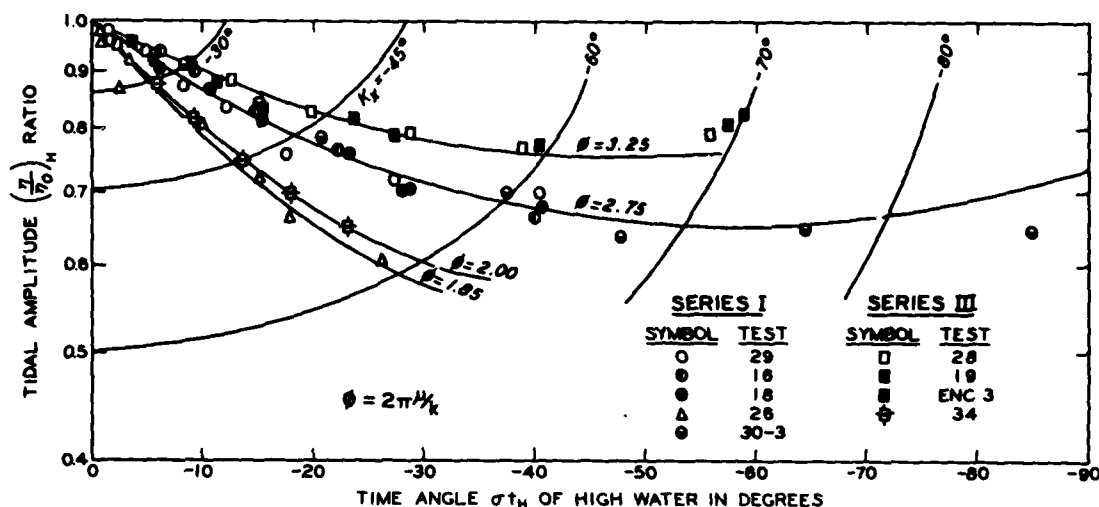lated in columns (4) and (8) are plotted as shown in fig. 6, and the value

Fig. 6. Determination of μ and k from tidal amplitudes
and time of high water

of ϕ (in equations 11 and 12) which best fits the experimental data is
found by trial. (In test 29, $\phi = 2.75$.) The value of kx for each ex-
perimental point along the ϕ = constant curve is interpolated from fig. 6
as shown in column (9) of table 2. Since the x distance (column 10) is
known for each point, the corresponding value of k is found as shown in
column (11) and the average value is used for the test. In test 29 this
average value is k = 0.186 degree/ft = 0.0033 radian/ft. From equation 10,
$\mu = \frac{\phi}{2\pi} k = \frac{2.75}{6.28}$ (0.0033) = 0.0014 radian/ft. The maximum value of the
tidal velocity at the ocean entrance as calculated from equations 21a and
22a is u_o = 0.44 ft/sec. Maximum velocities at other stations along the

channel were also calculated in the same manner. The variation of u_{max}
along the channel, as determined from the damped co-oscillating tidal

theory, is shown as the solid curve
in fig. 7. Also shown is the linear
velocity approximation (equation
39); within the region of salinity
intrusion the two curves agree
quite well. For test 29 vertical
velocity distributions were meas-
ured on the center line of the flume
at stations 5, 80, and 160 ft from
the ocean entrance. A comparison of
the experimental velocities at these
stations is shown in fig. 7. The

Fig. 7. Comparison of experimental
and calculated maximum velocities
along channel

points plotted are 88 per cent of the maximum average vertical center-line
velocities. This factor accounts for the velocity variation in the trans-
verse direction and was determined by averaging velocity measurements in
some of the preliminary flume tests.

55. Fig. 6 also shows the data from several other runs in series I
(tidal amplitude = 0.05 ft) and series III (tidal amplitude = 0.10 ft).
All of the pertinent tidal data are summarized in table 3. For all prac-
tical purposes μ and k may be considered to be quite independent of
changes in salinity and fresh-water velocity. The damping factor μ in-
creases with increasing tidal amplitude and decreasing tidal period (test
30-3). These changes in μ due to changes in tidal amplitude and period
are attributed to the assumption of linear frictional damping.

56. The roughness indicated in table 3 as side, bottom, and smooth
refers to the following conditions:

> Side roughness, 1/4-in. lucite strips on sidewalls only,
> spaced on 2-in. centers (n = 0.020)

> Bottom roughness, 1/4-in. lucite strips on bottom only,
> spaced on 2-in. centers (n = 0.018)

> Smooth, no roughness strips (n = 0.011)

The indicated values of Manning's n were based on measurements with
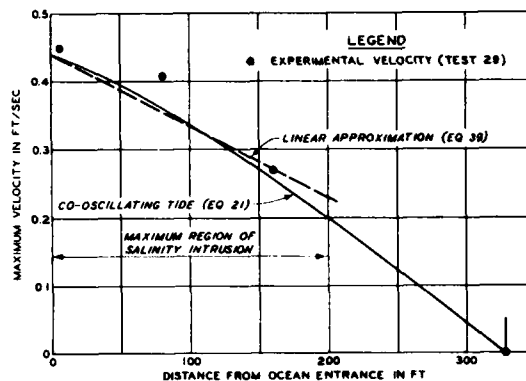fresh water under steady-flow conditions. For the series III tests,

table 3 shows that the value of μ changes in direct proportion to the change in n.

57. It is concluded that the values of μ and k as determined herein accurately reflect the effect of the various independent quantities on the tidal dynamics. The length and celerity of the tidal wave are also given in table 3. Both λ and c show a reduction, in comparison with the frictionless values λ_o and c_o, of approximately 75 per cent.
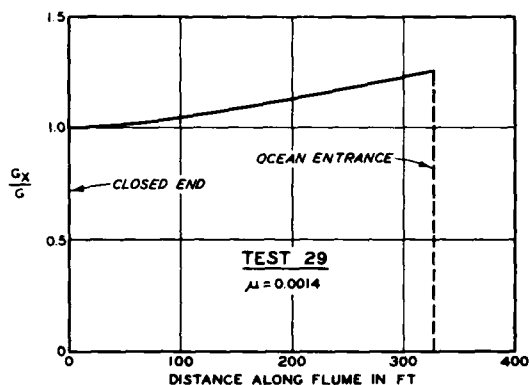
58. The value of the rate of energy dissipation (per unit mass of fluid), G, due to tidal friction is calculated from equation 26 and is also given in table 3. Fig. 8 shows a plot of the rate of energy dissipation in successive portions of the channel divided by the total rate. Within the region of salinity intrusion this ratio is reasonably constant.

Fig. 8. Variation of accumulated rate of energy dissipation along channel

Determination of Apparent Diffusion Coefficient and Boundary Conditions at Ocean Entrance

59. The fictitious length B marks the seaward extension of the channel to a point at which the salinity is constant at all times in the tidal cycle. This distance is evaluated by assuming that the salinity-convection function given by equation 40 also holds in this portion. It is observed that at the ocean entrance to the channel there is a fairly well-defined time interval β between the time of low water in the ocean and the time at which the ocean salinity first appears at the entrance on the flood tide. This is shown graphically in fig. 9 (test 15) in which the variation of mean salinity with time is shown for the test station nearest the ocean entrance ($x = 5$ ft). With the time interval β thus known, the distance B is calculated from equation 40 by noting that the salinity at low tide ($t/T = 0$) at $x = -B$ is equal to the salinity at $t/T = \beta$ at $x = +5$ ft. Hence,
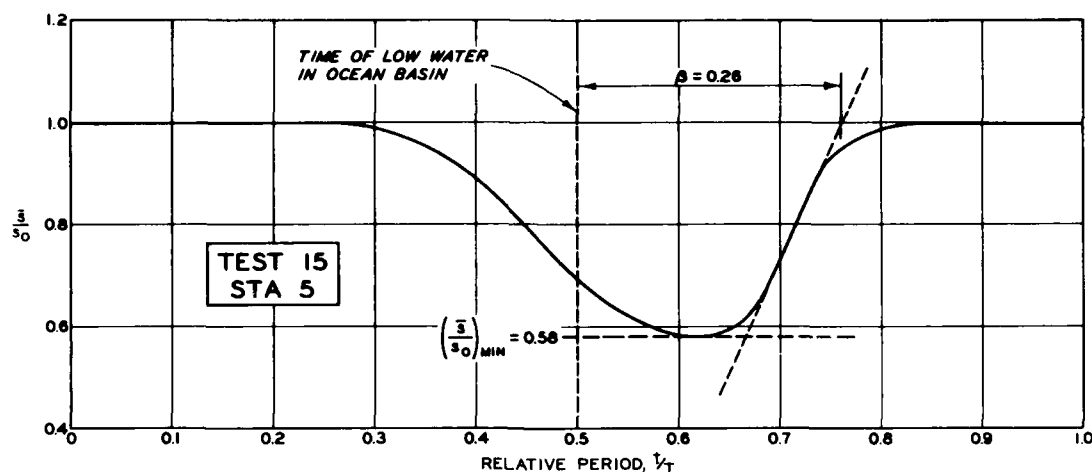
Fig. 9. Experimental salinity versus time curve for determination
of time interval β and minimum salinity

$$(1 + \delta B)\ e^{-a/h} = (1 - 5\delta)\ e^{-a/h(\cos 2\pi\beta)} \tag{52}$$

from which,

$$B = \frac{1}{\delta}\left[(1 - 5\delta)\ e^{a/h(1 - \cos 2\pi\beta)}\right] \tag{53}$$

The constant W in the low-tide salinity distribution equation 45 can be calculated by observing the _minimum salinity_ at the station nearest the ocean entrance ($x = 5$ ft), also shown in fig. 9. From equation 45,

$$\ln\left(\frac{\bar{s}}{s_o}\right)_{min} = -W(x_L + B)^2$$

hence, with $x = 5$,

$$W = \frac{U}{2D_o' B} = -\frac{\ln\left(\dfrac{\bar{s}}{s_o}\right)_{min}}{(5 + B)^2}$$

and

$$D_o' = \frac{U(5 + B)^2}{2B\left[-\ln\left(\dfrac{\bar{s}}{s_o}\right)_{min}\right]} \tag{54}$$

60. All of the quantities required to calculate the instantaneous salinity distributions given by equation 47 have been determined. In addition, the maximum and minimum intrusion lengths, equations 50 and 51, may be calculated. For each test the values of β, B, $(\bar{s}/s_o)_{min}$, and D'_o are tabulated in table 4.

Comparison of Experimental and Analytical Salinity Distributions

61. A graphical comparison of the calculated and experimental instantaneous salinity distributions at 10 per cent time intervals throughout the tidal cycle is given for test 15 in fig. 10. The agreement, especially for the maximum and minimum intrusion lengths is considered satisfactory.
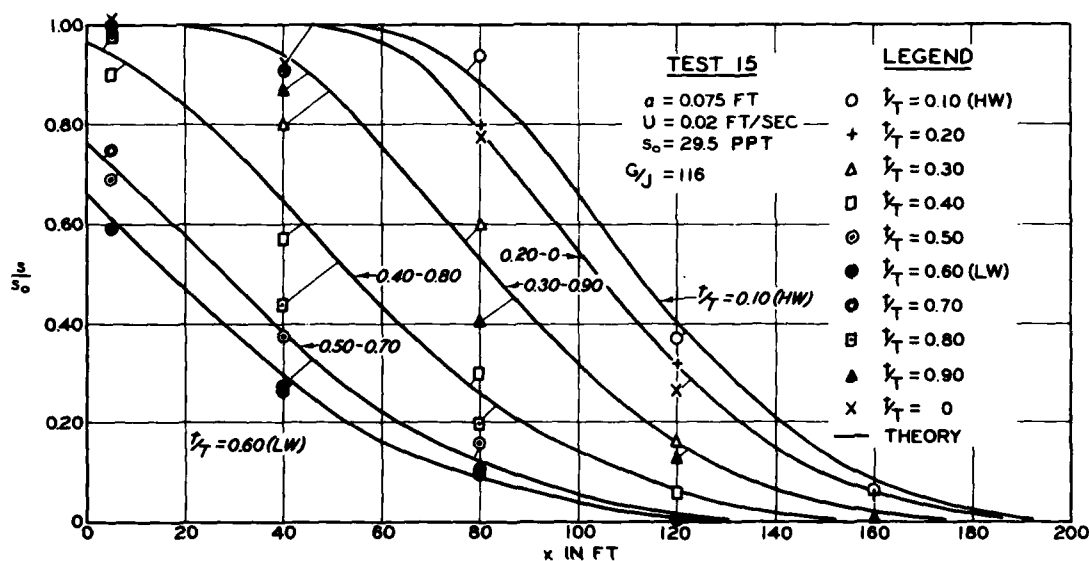

Fig. 10. Comparison of experimental and analytical instantaneous salinity distributions for a tidal cycle

62. In the following sequence of figures (figs. 11-15) the experimental and analytical salinity distribution comparisons for other tests are given for both high-water (HW) and low-water (LW) conditions. In these plots, the analytical salinity distribution is defined by the curves and the experimental salinity distribution by the plotted points. Fig. 11 shows the maximum and minimum salinity distributions for tests 16, 2, and 11 (series I). This group of tests shows the influence of the fresh-water
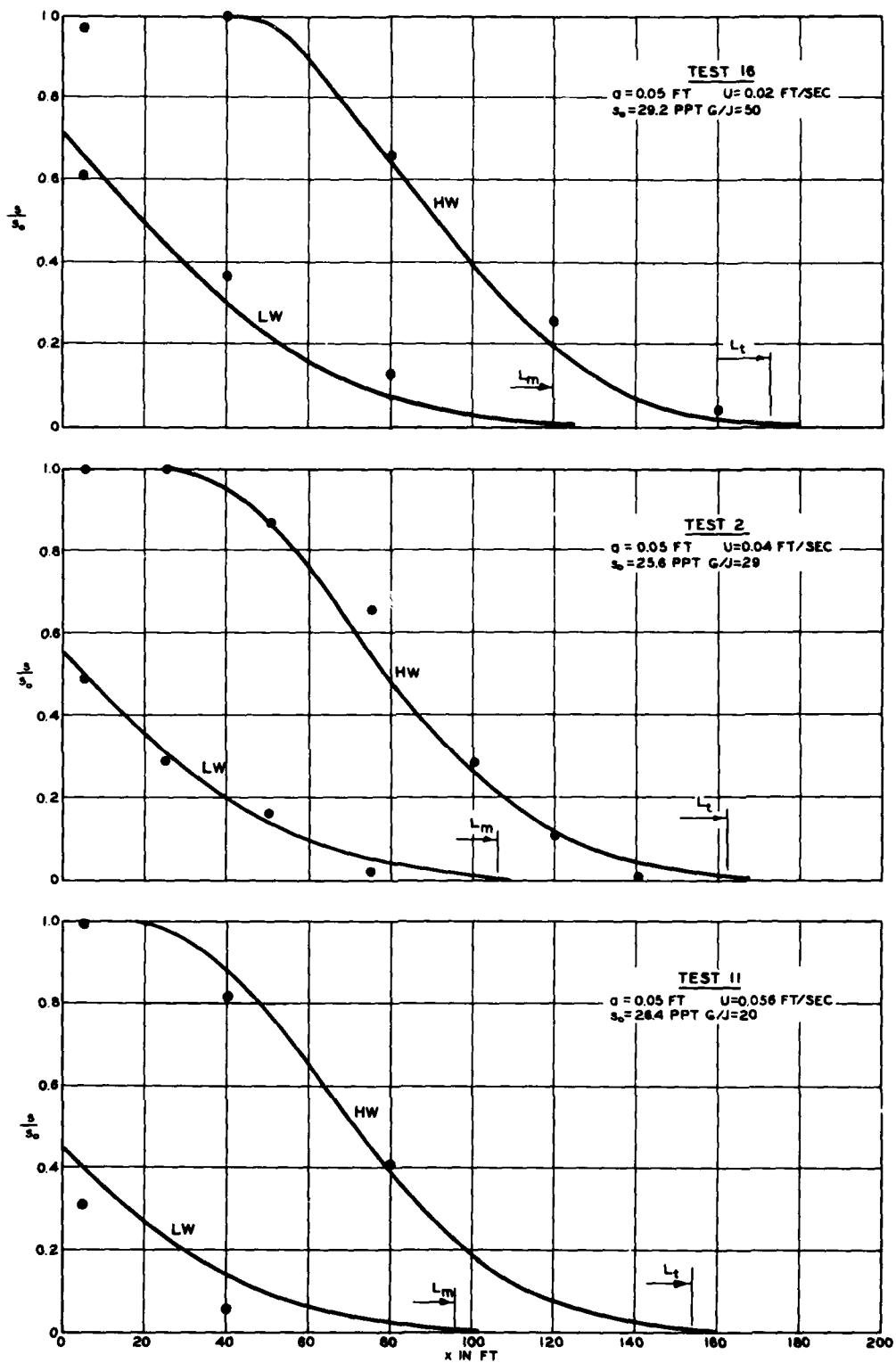
Fig. 11. Comparison of experimental and analytical salinity
distributions for series I, tests 16, 2, and 11

discharge which increases in the three tests in proportion to 1:2:2.8, all other conditions being constant. Results of the remaining tests of series I (18 and 26) are shown in fig. 12. Aside from a slight roughness change, the primary variable in these two tests is the ocean
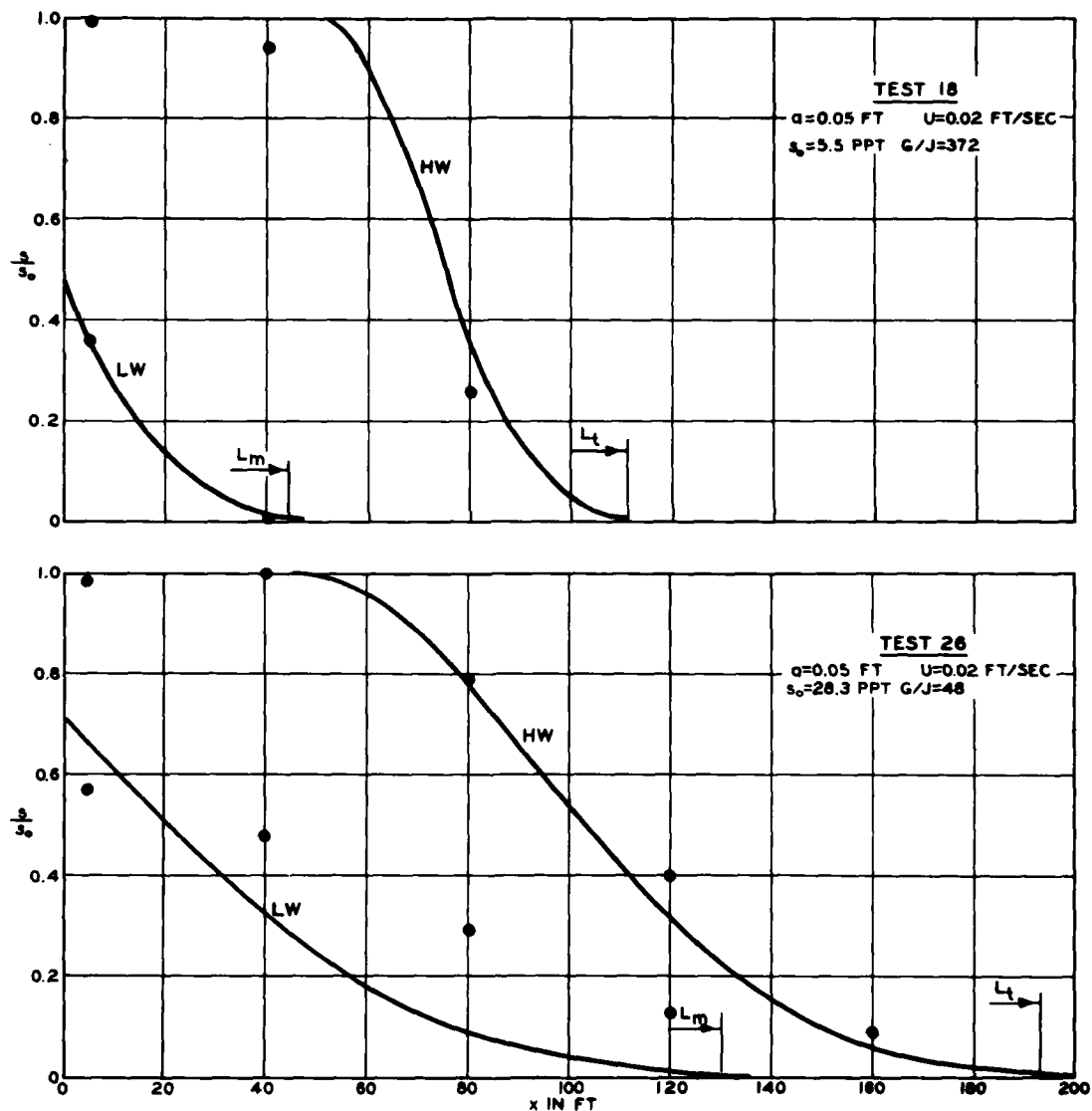

Fig. 12. Comparison of experimental and analytical
salinity distributions for series I,
tests 18 and 26

salinity which is approximately five times larger in test 26 than in test 18.

63. The two tests (15 and 10) in series II are shown in fig. 13 for different fresh-water flow rates and tidal amplitudes 50 per cent
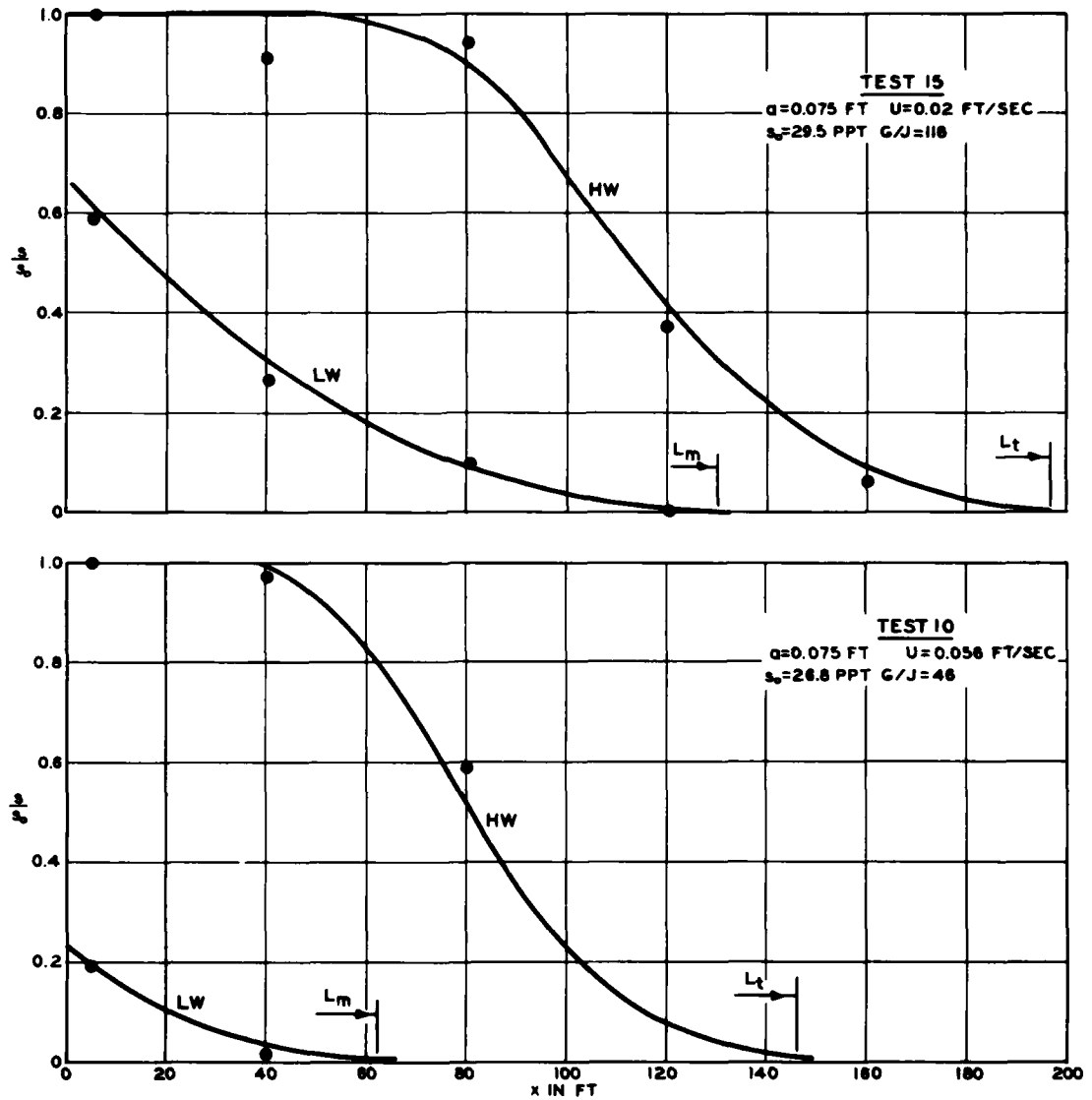

Fig. 13. Comparison of experimental and analytical
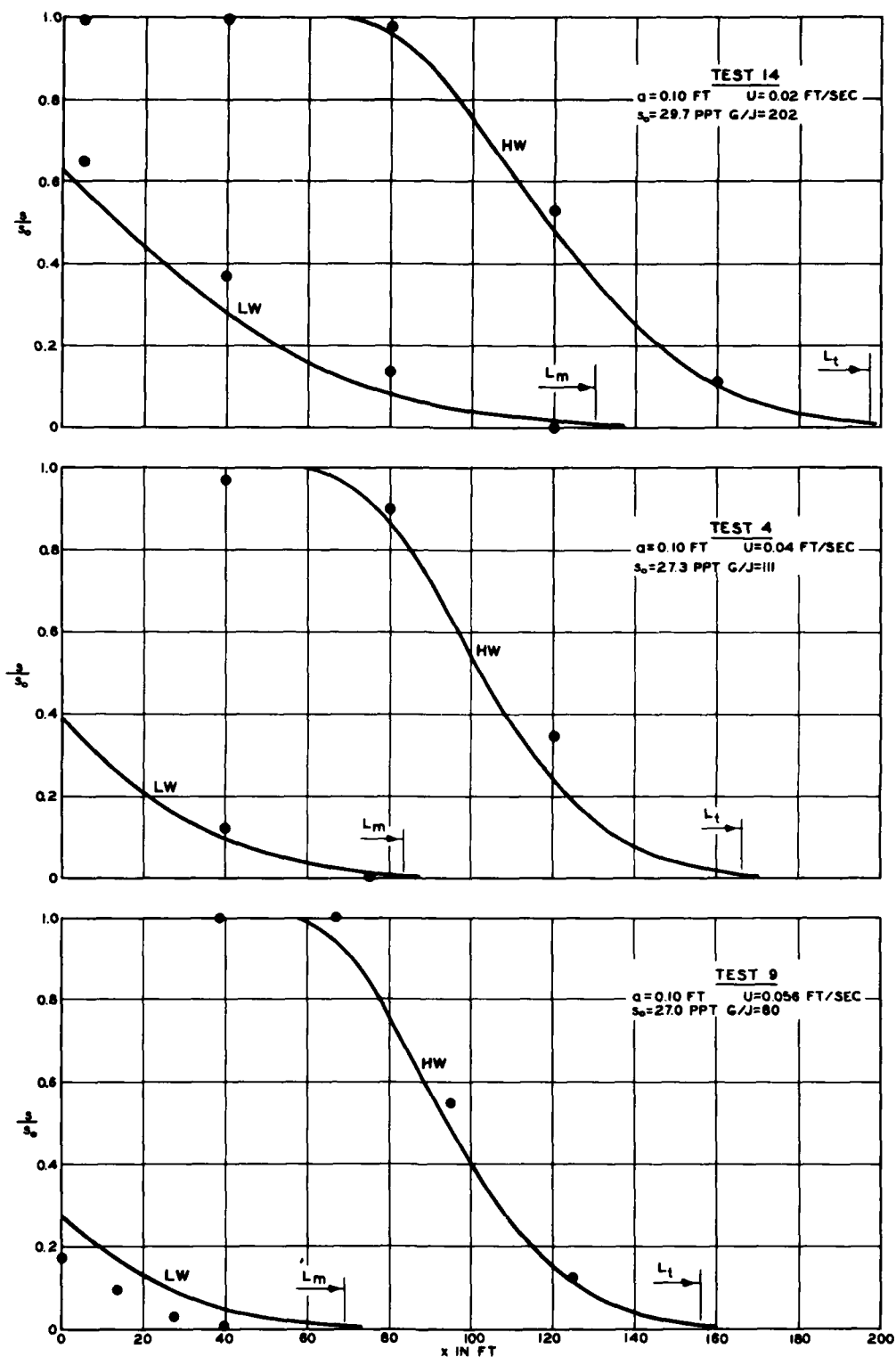salinity distributions for series II,
tests 15 and 10

Fig. 14. Comparison of experimental and analytical salinity
distributions for series III, tests 14, 4, and 9

greater than those of series I. Fig. 14 gives a sequence of three tests (14, 4, and 9) in series III (tidal amplitude twice as large as those of series I) for increasing fresh-water flow rates. Finally, tests 19 and 34 in fig. 15 show effects of ocean salinity and roughness change to complete the series III tests. In all cases the calculated and experimental salinity distributions are in reasonable agreement.
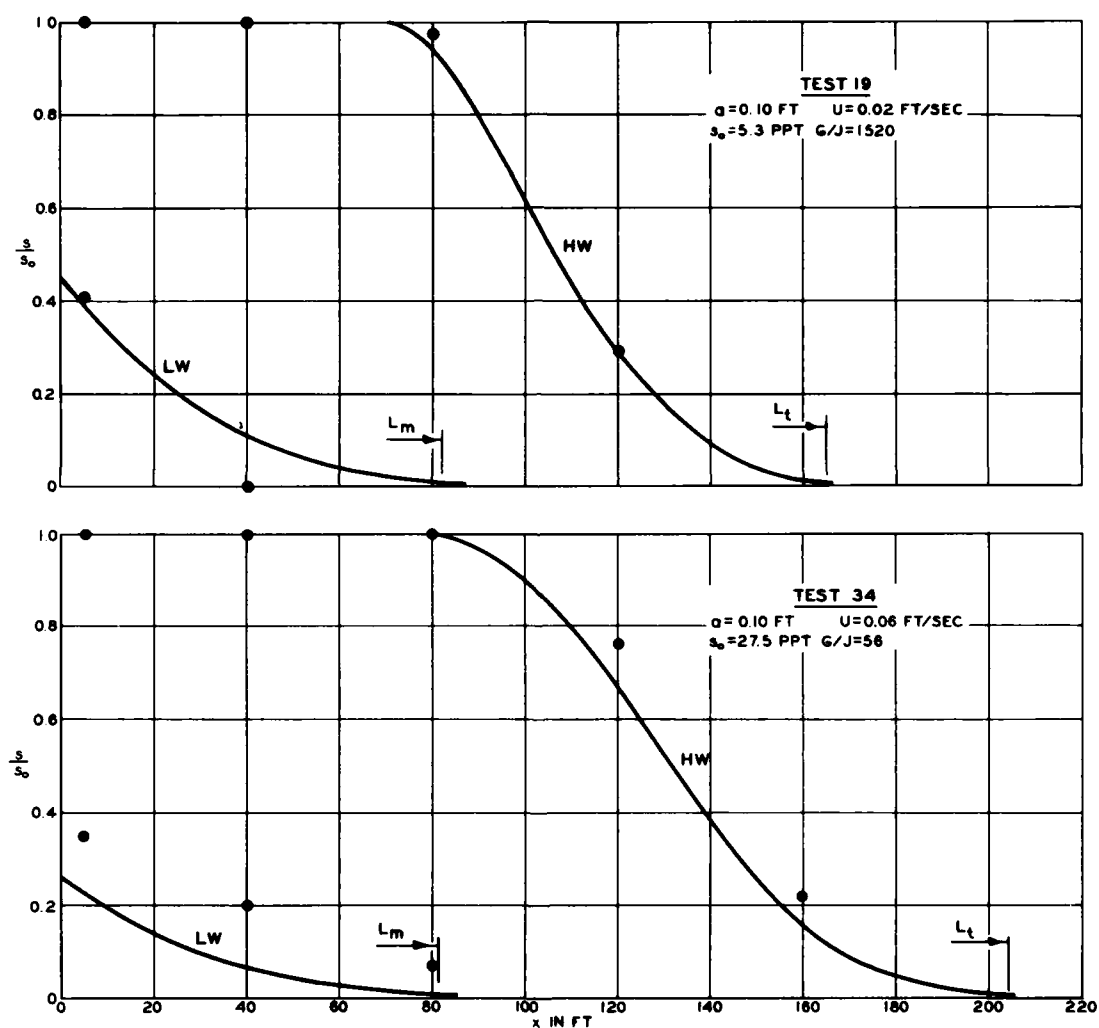

Fig. 15. Comparison of experimental and analytical
salinity distributions for series III,
tests 19 and 34

PART IV: CORRELATION OF DIFFUSION PARAMETERS

64. The determination of the instantaneous salinity distribution is
dependent upon two basic parameters: the apparent diffusion coefficient
at the channel entrance D_o' and the seaward excursion distance B . Both
quantities can be determined from an experimental record of the salinity
variation over a tidal cycle <u>at the flume entrance.</u> However, for a more
complete understanding, a correlation between D_o' , B , and the independent
quantities defined by equation 1 is required.

65. One relation is immediately obtained from the Kolmogoroff
theorem[10] relating the eddy diffusivity D_x to the rate of energy dissi-
pation per unit mass of fluid G and the mean eddy size ℓ .

$$D_x = (\text{constant})\ G^{1/3}\ \ell^{4/3} \tag{55}$$

If the scale of turbulence ℓ is a function of the physical dimensions of
the system and is assumed to be constant, the eddy diffusivity should vary
in proportion to $G^{1/3}$.

66. Tests 31, 32, and 33 in the WES flume were conducted using dyed
fresh water in place of the saline ocean water. The dye concentration was
of the order of 1 ppm and density differences were therefore negligible.
The coefficients obtained are thus true eddy diffusivities unaffected by
gravitational convection. From table 4 it is seen that for tests 32 and
33 the ratio $D_o/G^{1/3}$ is equal to a constant 2.8 (D_o for test 31 could
not be obtained due to a lack of definition of the experimental concentra-
tion curve). It is also noted that the ratio $D_o'/G^{1/3}$ for all other tests
employing saline water is greater than 2.8. This ratio reaches a maximum
value of 25 for test 11 which represents the maximum fresh-water discharge
and maximum ocean salinity for the minimum tidal range (i.e. the most
highly stratified condition).

67. The above observations are illustrated in fig. 16 which is a
plot of D_o' and D_o versus the cube root of the tidal energy dissipation
rate G . The zero-density runs plot as a straight line indicating that
D_o is directly proportional to $G^{1/3}$. In other words the transfer of
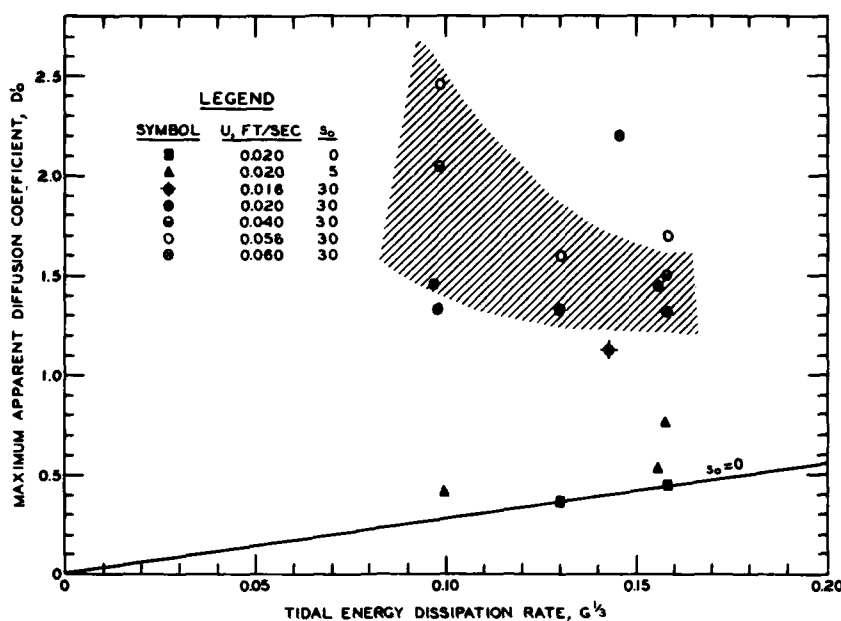salt upstream by turbulent diffusion increases with the rate of tidal

Fig. 16. Diffusion coefficient versus rate of tidal energy dissipation

energy dissipation. The saline tests exhibit the opposite trend, a non-linear, inverse relation between D_0' and $G^{1/3}$. As the energy dissipation (and therefore the turbulence) increases, the transfer of salt up-stream by the combined processes of gravitational convection and diffusion decreases. This trend is indicated by the shaded region in fig. 16 and shows that as the turbulent mixing increases, the gravitational convection of salt is reduced. A measure of the partially mixed estuary is the ratio of the apparent diffusion D_0' (due to the combined salt-transfer processes) to the turbulent diffusion coefficient D_0 . Hence, from equation 55

$$\frac{D_0'}{D_0} \sim \frac{D_0'}{G^{1/3}}$$

68. The ratio $D_0'/G^{1/3}$ is seen to be a significant expression of the increase in salt transfer due to gravitational convection. Hence, it would be expected to correlate with some function involving the density difference between the fresh water and the ocean. In the MIT tests (reference 10) such a correlation was found between $D_0'/G^{1/3}$ and a dimensionless parameter of the following form:

$$\frac{G}{J} = \frac{\text{rate of energy dissipation per unit mass of fluid}}{\text{rate of potential energy gain per unit mass of fluid}}$$

The gain in potential energy (per unit volume), as water moves down the estuary toward the sea, is due to its increasing specific weight, i.e. $\Delta\gamma h \left(\frac{\text{ft-lb}}{\text{ft}^3}\right)$, where $\Delta\gamma$ = difference in specific weight of fresh water and ocean; thus, the gain in potential energy per unit mass is therefore

$$\frac{\Delta\gamma h}{\rho} = \left(g\,\frac{\Delta\gamma}{\gamma}\right)h\left(\frac{\text{ft-lb}}{\text{mass}}\right)$$

Since the average time of retention of the fresh water in the estuary is $t_r = \frac{L}{U}$, the time average rate of gain of potential energy per unit mass of fluid is given by

$$J = \frac{g\,\frac{\Delta\gamma}{\gamma}\,h}{t_r} = \frac{g\,\frac{\Delta\gamma}{\gamma}\,hU}{L} \tag{56}$$

Hence, from equation 26

$$\frac{G}{J} = \frac{1}{2}\frac{c}{U}\left(\frac{a}{h}\right)^2\frac{M}{\Delta\gamma/\gamma} \tag{57}$$

where the tidal wave celerity $c = \sigma/k$ and

$$M = \frac{\sinh 2\mu L}{\cos 2kL + \cosh 2\mu L} \tag{58}$$

The values of G/J are tabulated in table 4. Fig. 17 is a plot of $D_o'/G^{1/3}$ versus G/J , and it is seen that a significant correlation of the apparent diffusion coefficient has been obtained in terms of the tidal and fresh-water flow characteristics of the estuary. The parameter G/J is analogous to a Richardson number which expresses the stability criterion for flows with vertical density gradients. The parameter is furthermore a quantitative measure of the degree of stratification or mixing in an estuary. Increasing values of G/J indicate increasingly well-mixed conditions; for the case of zero gravitational effects, G/J approaches infinity.

69. The remaining problem in the one-dimensional treatment is to find a correlation between the seaward excursion (defined by the fictitious
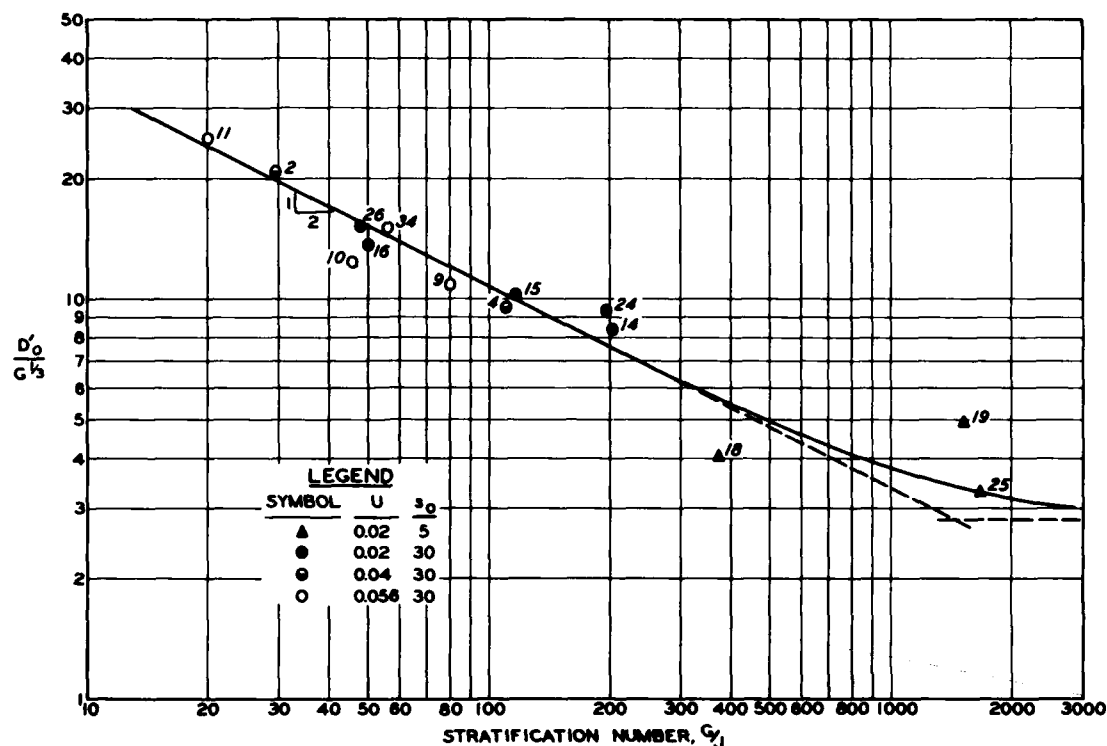
Fig. 17. Correlation of apparent diffusion coefficient D_o'
with stratification number

length B) and the independent quantities of the system. Fig. 9 shows the
time variation of the salinity at the ocean entrance of the flume. It is
noted that full ocean salinity exists at this point during approximately
one-half the tidal cycle and that during the other half of the cycle the
average salinity is reduced. The physical explanation is that (during the
major portion of the flood tide) the fresh-water inflow is stored in the
estuary. On the ebb cycle the removal of the fresh water causes a dilu-
tion as indicated by the observed salinity curve. It is apparent from
equation 53 that the time lag β and therefore the parameter B are de-
pendent on the shape of the salinity versus time curve at the flume
entrance.

70. The shape of this curve is given by equation 47; with $x = 0$,

$$\frac{s(o,t)}{s_o} = \exp\left\{ - \frac{U}{2\,D_o'\,B\,\delta^2} \left[1 - e^{a/h(1 - \cos \sigma t)} + \delta B \right]^2 \right\} \qquad (59)$$

42

If a/h is small compared to unity, the exponential term

$$e^{a/h(1 - \cos \sigma t)} \cong 1 + \frac{a}{h} (1 - \cos \sigma t)$$

and since $\delta = \dfrac{a\sigma}{hu_o}$, equation 59 may be written

$$\frac{s(o,t)}{s_o} = \exp\left\{ - \frac{UB}{2D_o'} \left[1 - \frac{u_o}{\sigma B} (1 - \cos \sigma t) \right]^2 \right\} \tag{60}$$

The salinity variation with time at the estuary entrance is therefore seen to be a function of two dimensionless parameters $\dfrac{UB}{D_o'}$ and $\dfrac{u_o}{\sigma B}$. The physical significance of the latter quantity may be given as follows: The tidal excursion is the average longitudinal distance traveled by a particle in a tidal cycle; this distance is proportional to $\dfrac{u_o T}{2}$ and since $\sigma = 2\pi/T$, tidal excursion $\sim \dfrac{u_o}{\sigma}$.

71. Therefore, $\dfrac{u_o}{\sigma B}$ is a parameter proportional to the ratio of the tidal excursion to the seaward excursion of salinity B . It has been found that this quantity is related to the stratification parameter G/J previously discussed.

72. Fig. 18 is a plot of $\sigma B/u_o$ versus G/J for all of the salinity

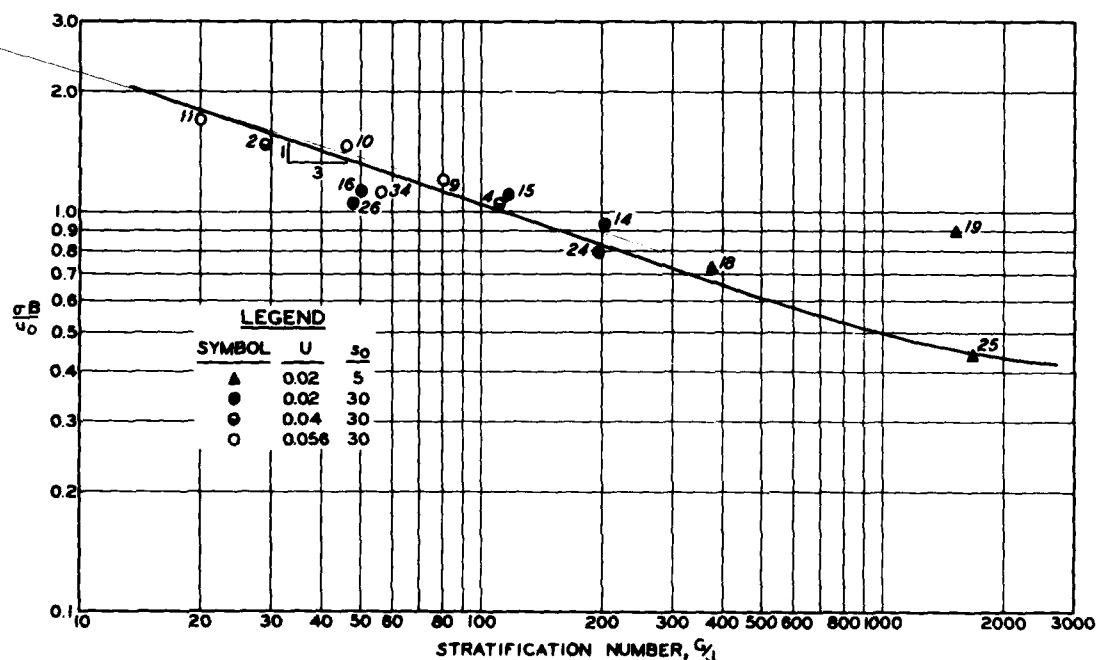Fig. 18. Correlation of seaward excursion distance B
with stratification number

tests tabulated in table 4. It is concluded that a reasonable correlation exists and that well-mixed conditions are characterized by small values of $\sigma B/u_o$.

PART V: CONCLUSIONS

Longitudinal Salinity Distribution in a Uniform Estuary

73. It is concluded that the objectives of the one-dimensional phase
of this investigation have been accomplished. Analytical expressions have
been developed to describe the instantaneous distribution of the mean ver-
tical salinity throughout the tidal cycle, and thus the maximum and minimum
salinity-intrusion lengths for the uniform estuary are also specified.

74. In general, the following independent quantities must be speci-
fied initially: estuary length, mean depth, ocean tidal amplitude, period,
ocean salinity concentration, and fresh-water discharge. The salinity dis-
tribution equations involve five basic quantities in addition to those
specified above: the tidal damping modulus μ , the tidal wave number
$k = 2\pi/\lambda$, the maximum tidal velocity at the ocean entrance u_0 , the ap-
parent diffusion coefficient at the ocean entrance D_0' , and the seaward
excursion B . The first three (μ , k , u_0), being exclusively tidal pa-
rameters, are determined from observations of the tidal elevations within
the estuary by means of the damped co-oscillating tidal theory developed
in paragraphs 18-32. This method of determining the tidal characteristics
from elevations (which in the case of actual estuaries are either already
known or readily measured) shows promise for future field studies.

75. It has been demonstrated that the remaining quantities D_0' and
B can be determined from an observation of the salinity variation with
time at the ocean entrance as shown in paragraphs 59-60. On the basis of
these determinations significant correlations have been developed between
D_0' , B , and the tidal and physical specifications of the estuary. In par-
ticular, D_0' and B are correlated with G/J , the ratio of the mean rate
of turbulent energy dissipation to the rate of increase of potential energy
(due to the change in salinity along the estuary). It is suggested that
this ratio be called the stratification number since it has been shown to
be a quantitative measure of the extent of vertical mixing in an estuary.

76. If use is made of the approximation $e^{-2a/h} = 1 - 2a/h$, the
equation (49) for the maximum salinity-intrusion length may be written:

$$L_t = \frac{2u_o}{\sigma} + \left(1 - \frac{2a}{h}\right) B \left(3\sqrt{\frac{D_o'}{UB}} - 1\right) \qquad (49a)$$

From the above it is seen that the intrusion length in a uniform estuary varies in a relatively complex manner with the various tidal and diffusion quantities. For the flume tests a quantitative evaluation of the influence of these quantities on the intrusion length may be made by comparing the values of L_t indicated in figs. 11-15.

77. Equation 49a may also be written in dimensionless form by using the tidal excursion parameter u_o/σ as a reference length; thus,

$$\frac{L_t}{u_o/\sigma} = 2 + \left(1 - \frac{2a}{h}\right)\left(\frac{\sigma B}{u_o}\right)\left(3\sqrt{\frac{D_o'}{UB}} - 1\right)$$

The ratio of the maximum salinity-intrusion distance to the tidal excursion therefore depends on three dimensionless quantities:

    <u>a</u>. a/h , the ratio of ocean tidal amplitude to estuary mean depth

    <u>b</u>. $\sigma B/u_o$, the ratio of the seaward salinity excursion to the tidal excursion

    <u>c</u>. D_o'/UB , the ratio of the diffusion distance D_o'/U to the seaward salinity excursion

The quantities D_o' and B are given in terms of the stratification number G/J in figs. 17 and 18. The stratification number can be evaluated from the tidal parameters a, σ , k , and μ ; the estuary length L and mean depth h ; the mean fresh-water flow rate U ; and the ocean water-fresh water specific weight difference $\Delta\gamma/\gamma$ as given by equation 57.

78. On the basis of the specific information presented in this study, it is possible to make quantitative predictions regarding salinity intrusions in partially or well-mixed estuaries of essentially uniform cross section <u>without prior knowledge of any existing salinity conditions</u>. In addition, the factors which cause changes in salinity intrusions have, for the first time, been quantitatively evaluated. Thus by means of the intrusion equations, the effect of changes in the fresh-water discharge, channel depth, etc., can be predicted. Of even greater importance is the possibility that the diffusion and tidal parameters developed as a result of this study will have important significance in understanding the intrusion mechanics of estuaries of nonuniform geometry.

Significance of the Stratification Number

79. Previous investigators of the problem of salinity intrusion in
tidal estuaries have proposed that the ratio of the volume of fresh-water
inflow in a tidal cycle to the tidal prism is an important parameter de-
scribing the mixing characteristics of the estuary. The tidal prism is de-
fined differently by various writers. In some cases it is defined as the
change in the volume of the estuary between low water and high water. In
other cases it has been taken equal to the volume of sea water entering
the estuary on the average flood tide. The latter definition differs from
the former in that it does not consider the volume of fresh-water inflow
during the flood cycle as part of the tidal prism. Another ambiguity
arises as to the meaning of the tidal prism where (as is almost always the
case) the time of high water or low water occurs at different times along
the estuary. According to the first definition, the tidal prism would be
the volume contained in the envelope between high- and low-water levels.
The objective of this discussion is to relate the stratification number to
the fresh water-tidal prism ratio. For this purpose the tidal prism is
taken as the volume of sea water entering the estuary on the flood tide.
If the tidal velocity at the estuary entrance varies harmonically with
time, the average velocity over a half cycle (flood tide) is $2/\pi$ times
the maximum; hence, the tidal prism P_t is

$$P_t = \frac{2}{\pi} u_o \, (bh) \, \frac{T}{2} = \frac{u_o \, bhT}{\pi}$$

The volume of fresh-water inflow during a full tidal cycle is

$$Q_f \, T = UbhT$$

Hence, the ratio

$$\frac{Q_f \, T}{P_t} = \frac{\pi U}{u_o}$$

This ratio is plotted against the stratification number in fig. 19.

80. From equation 57 it can be seen that for a given estuary in
which the only variable is the fresh-water velocity U , the stratification
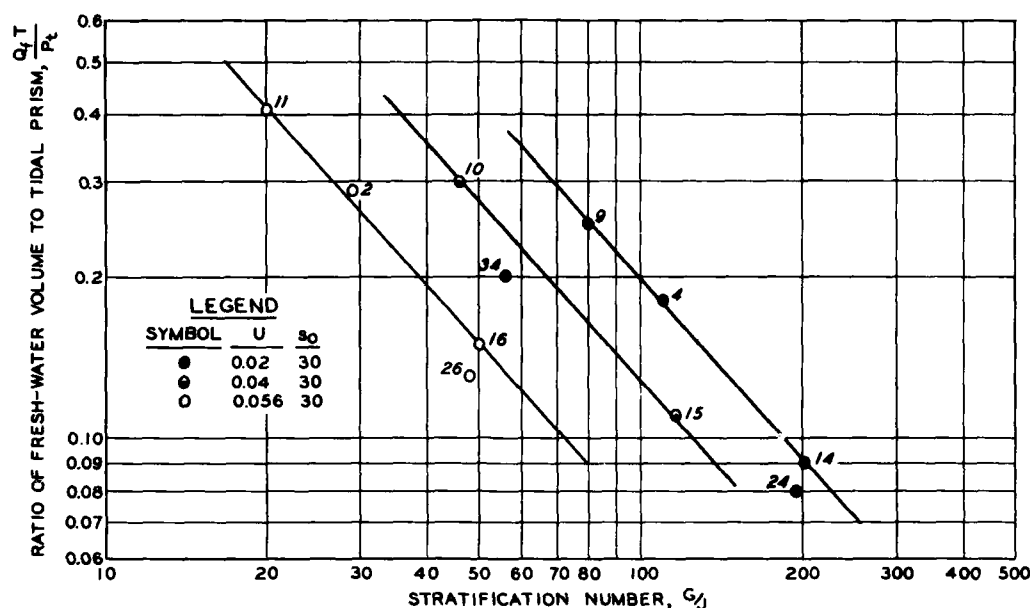
Fig. 19. Relation between fresh-water volume:tidal prism ratio
and stratification number

number G/J is proportional to 1/U . The tidal prism ratio under these
conditions is proportional to U ; therefore, it would be expected that
for a sequence of runs in which only U is varied, the relation between
the two parameters would be linear in logarithmic coordinates. Fig. 19
shows the expected result for the test sequences (11, 2, 16), (10, 15),
and (9, 4, 14). The important conclusion is that the tidal prism ratio is
not indicative of the extent of mixing if any other quantity such as tidal
amplitude, depth, or roughness is a variable. In other words, equal values
of the tidal prism ratio do not necessarily indicate similar mixing condi-
tions; however, equal values of the stratification number do indicate
similar conditions. This conclusion is demonstrated by fig. 20 which
shows on a dimensionless basis the vertical salinity gradients for tests
11, 10, 16, and 14. The plotted profiles are for a station 40 ft from the
ocean tidal basin and correspond to the conditions existing at approxi-
mately one-quarter of a tidal cycle after the time of high water in the
basin, at which time the vertical salinity gradients for all runs are a
maximum. Fig. 20 clearly indicates the correlation between the stratifica-
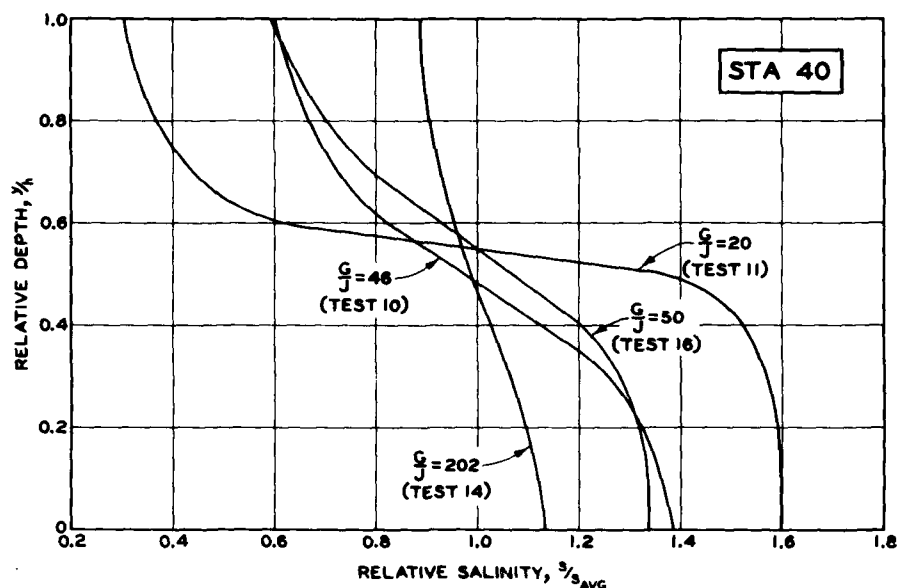tion number and the vertical salinity gradient. Test 11 (G/J = 20) is the

Fig. 20. Vertical salinity gradients in relation
to stratification number

most stratified and test 14 (G/J = 202) the least stratified of all the
runs with 30 ppt salt in the ocean basin. Of particular interest here is
that tests 10 and 16 are from different series, with test 16 having two-
thirds the tidal amplitude and one-third the fresh-water flow rate of test
10. The stratification numbers for these two tests are approximately the
same, and the vertical salinity gradients as shown in fig. 20 are also
similar. The values of the tidal prism ratio, however, differ by a factor
of two as is readily verified from fig. 19.

81. It is concluded that the stratification number is sensitive to
the various factors affecting the salinity regime in a uniform estuary.
The tidal prism ratio is sensitive only to changes in fresh-water flow,
all other conditions being equal.

PART VI: RECOMMENDATIONS

82. It is proposed that the general investigation of salinity in-
trusion be continued along the lines of the four-phase program originally
outlined by the Tidal Hydraulics Committee (see Preface). It is suggested
that the second and third phases, i.e. the vertical mixing of fresh and
salt water, the resulting vertical salinity distribution, and the vertical
distribution of current velocities as affected by salinity distribution, be
treated as a single unit. In essence, the second and third phases imply a
two-dimensional analysis of the salinity-intrusion problem, and they are a
logical extension of the one-dimensional analysis treated in this report.

83. Recent research in the MIT Hydrodynamics Laboratory under non-
tidal conditions (reference 7) and earlier field investigations by Prit-
chard in the James River have shown the feasibility of a two-dimensional
analysis. Vertical velocity distributions can be derived from horizontal
and vertical salinity gradients through the conservation-of-mass equation.
The time average vertical velocity distributions are of the familiar "s"
shape with a seaward flow near the surface and a landward flow near the
bottom. The MIT tests, for a range of partially mixed conditions, showed
surprisingly large magnitudes of the ratio of landward bottom velocity to
average vertical velocity. Of particular interest is the fact that a rela-
tion seems to exist between this local bottom velocity ratio and the local
densimetric Froude number. The densimetric Froude number is based on the
fresh-water velocity, depth, and local density difference $\Delta\rho_x/\rho$. In the
landward direction, this quantity increases (since $\Delta\rho_x/\rho$ is in the de-
nominator) and the bottom velocity decreases. These results are obtained
in the case of a steady-state salinity distribution in homogeneous turbu-
lence. The experimental data already obtained in the WES flume can be
analyzed in a similar manner. More specific information on variations of
the landward bottom velocity or flow predominance along an estuary should
be useful in view of its demonstrated importance to sediment movement and
deposition. This leads directly to the fourth phase of the general study.

84. As a parallel investigation it is also recommended that the one-
dimensional approach, as contained in this report, be broadened to include
a study of the longitudinal distribution of salinity in an estuary of

nonuniform geometry. For this purpose available test data from the modi-
fied Delaware estuary model could be utilized to advantage.

REFERENCES

1. Arons, A. B., and Stommel, H., "Mixing length theory of tidal flushing." _Transactions, American Geophysical Union,_ vol 32, No. 3 (June 1951), pp 419-421.

2. Defant, A., "Gezeiten Probleme des Meeres in Landnahe." _Probleme der Kosmischen Physik,_ vol VI, Hamburg (1925), pp 1-80.

3. Dronkers, J. J., and Schoenfeld, J. C., "Tidal computations in shallow water." _Proceedings, American Society of Civil Engineers,_ vol 81, Separate No. 714 (June 1955).

4. Einstein, H. A., and Fuchs, R. A., _The Prediction of Tidal Flows in Canals and Estuaries._ First Report to the Committee on Tidal Hydraulics (Corps of Engineers), 1954.

5. Fjeldstad, J. E., "Contributions to the dynamics of free progressive tidal waves, Norwegian North Polar Expedition with the MAUD (1918-1925)." _Scientific Results,_ vol 4, No. 3.

6. Harleman, D. R. F., Jordaan, J. M., and Lin, J. D., _The Diffusion of Two Fluids of Different Density in a Homogeneous Turbulent Field._ MIT Hydrodynamics Laboratory, Technical Report No. 31, February 1959.

7. Harleman, D. R. F., McDougall, D. W., and Galvin, C. J., _An Analysis of Two-dimensional Convective Diffusion Phenomena in an Idealized Estuary._ MIT Hydrodynamics Laboratory, Technical Report No. 42, January 1961.

8. Hildebrand, F. B., _Advanced Calculus for Engineers._ Prentice-Hall, Inc., Englewood Cliffs, N. J., 1949.

9. Ippen, A. T., and Harleman, D. R. F., _Investigation on Influence of Proposed International Passamaquoddy Tidal Power Project on Tides in the Bay of Fundy._ Report to New England Division, Corps of Engineers, July 1958.

10. Ippen, A. T., Harleman, D. R. F., and Lin, J. D., _Turbulent Diffusion and Gravitational Convection in an Idealized Estuary._ MIT Hydrodynamics Laboratory, Technical Report No. 38, March 1960.

11. Ketchum, B. H., "The exchange of fresh and salt water in tidal estuaries." _Journal of Marine Research,_ vol 10 (1951).

12. Perroud, P., _The Propagation of Tidal Waves into Channels of Gradually Varying Cross Section._ University of California I. E. R. Series 89, Issue 3, October 1958.

52

13. Pritchard, D. W., "Estuarine circulation patterns." _Proceedings,_
    American Society of Civil Engineers, vol 81, Separate No. 717 (June
    1955).

14. Redfield, A. C., "The analysis of tidal phenomena in narrow embay-
    ments." _Papers in Physical Oceanography and Meteorology,_ No. 529,
    MIT and Woods Hole Oceanographic Institution, vol XI, No. 4 (1950),
    pp 1-36.

15. Sverdrup, H. U., Johnson, M. W., and Fleming, R. H., _The Oceans:_
    Their Physics, Chemistry, and General Biology. Prentice-Hall, Inc.,
    Englewood Cliffs, N. J., 1942.

16. U. S. Army Corps of Engineers, _Evaluation of the Present State of_
    Knowledge of Factors Affecting Tidal Hydraulics and Related Phenomena.
    Committee on Tidal Hydraulics Report No. 1, February 1950.

17. U. S. Army Engineer Waterways Experiment Station, _Investigation of_
    Salinity and Related Phenomena (Interim Report on Flume Control
    Tests). Vicksburg, Miss., January 1955.

Table 1

Summary of Flume Tests Used in Analysis

Flume depth at msl = 0.5 ft   Tidal period = 600 sec (except 30-3)
Length of flume = 327 ft   Flume width = 0.75 ft

Test No.	Tidal Amplitude ft	Nominal Source Salinity ppt	Fresh-water Discharge cfs	Flume Rough-ness	Comments
			Series I		
29	0.05	0	0	Side	
30-3	0.05	0	0	Side	Tidal period changed to 420 sec
18	0.05	5	0.0075	Side	
16	0.05	30	0.0075	Side	
2	0.05	30	0.0150	Side	
11	0.05	30	0.0210	Side	
26	0.05	30	0.0075	Bottom	Similar to test 16 but roughness changed
31	0.05	0 (dye)	0.0075	Side	Fresh water in tidal basin with dye as tracer
			Series II		
15	0.075	30	0.0075	Side	
10	0.075	30	0.0210	Side	
32	0.075	0 (dye)	0.0075	Side	Fresh water in tidal basin with dye as tracer
			Series III		
28	0.10	0	0	Side	
19	0.10	5	0.0075	Side	
14	0.10	30	0.0075	Side	
4	0.10	30	0.0150	Side	Limited experimental data
9	0.10	30	0.0210	Side	Limited experimental data
25	0.10	5	0.0075	Bottom	Similar to test 19 but roughness changed
24	0.10	30	0.0075	Bottom	Similar to test 14 but roughness changed
34	0.10	30	0.0225	Smooth	
33	0.10	0 (dye)	0.0075	Side	Fresh water in tidal basin with dye as tracer

Table 2

Tidal Analysis, Test 29

(1) Distance from Ocean Entrance ft	(2) η ft +msl		(3) $\eta_{H_{avg}}$ ft +msl	(4) $\dfrac{\eta_H}{\eta_{oH}}$	(5) $\dfrac{t}{T}$		(6) $\left(\dfrac{t_M}{T}\right)_{avg}$	(7) $\left(\dfrac{t_H}{T}\right)_{avg}$	(8) σt_H, degrees $360°(7)$	(9) kx, degrees $\phi = 2.75$	(10) x ft	(11) k degree/ft
1	HW +0.047	LW -0.054	0.050	0.70	HW 0.017	LW 0.482	-0.001	-0.112	-40.3	-61	-326	0.187
40	+0.051	-0.053	0.052	0.72	0.042	0.528	0.035	-0.076	-27.3	-54	-287	0.188
80	+0.052	-0.058	0.055	0.76	0.070	0.555	0.062	-0.049	-17.6	-46	-247	0.186
120	+0.058	-0.063	0.060	0.84	0.073	0.583	0.078	-0.034	-12.2	-38	-207	0.184
160	+0.063	-0.063	0.063	0.875	0.085	0.592	0.088	-0.023	-8.3	-32	-167	0.191
200	+0.067	-0.068	0.068	0.94	0.090	0.605	0.097	-0.014	-5.0	-23	-127	0.181
240	+0.068	-0.071	0.069	0.96	0.100	0.612	0.106	-0.005	-1.8	-18	-87	0.205
280	+0.071	-0.071	0.071	0.99	0.100	0.623	0.111	0	0	---	-47	---
320	+0.071	-0.073	0.072	1.00	0.100	0.623	0.111	0	0	---	-7	---

Note: k_{avg} = 0.186 degree/ft.

Table 3

General Summary of Tidal Characteristics

Mean depth, h = 0.5 ft

Tidal period, T = 600 sec (except where noted)

σ = 0.010 1/sec

Length, L = 327 ft

Width, b = 0.75 ft

$c_o = \sqrt{gh}$ = 4.0 ft/sec

$\lambda_o = c_o T$ = 2400 ft

k_o = 0.0026 radian/ft

Test No.	Roughness	s_o ppt	U ft/sec	k radian/ft	μ radian/ft	$\lambda = \frac{2\pi}{k}$ ft	$c = \frac{\lambda}{T}$ ft/sec	$G \times 10^3$ ft²/sec³	u_o ft/sec	δ 1/ft
				Series I, Tidal Amplitude = 0.05 ft						
29	Side	0	0	0.0033	0.0014	1925	3.18	--	0.44	--
30-3*	Side	0	0	0.0048	0.0021	1350	3.12	--	0.48	--
18	Side	5.5	0.02	0.0035	0.0015	1790	3.00	1.00	0.43	0.0024
16	Side	29.2	0.02	0.0034	0.0015	1860	3.08	0.95	0.43	0.0024
2	Side	25.6	0.04	(T16)	(T16)	(1860)	(3.08)	(0.95)	(0.43)	(0.0024)
11	Side	26.4	0.056	(T16)	(T16)	(1860)	(3.08)	(0.95)	(0.43)	(0.0024)
26	Bottom	28.3	0.02	0.0032	0.0014	1940	3.28	0.88	0.49	0.0021
31	Side	Dye	0.02	(29)	(T29)	(1925)	(3.18)	(0.93)	(0.44)	--
				Series II, Tidal Amplitude = 0.075 ft						
15	Side	29.5	0.02	0.0035	0.0017	1790	3.00	2.20	0.59	0.0026
10	Side	26.8	0.056	(T15)	(T15)	(1790)	(3.00)	(2.20)	(0.59)	(0.0026)
32	Side	Dye	0.02	(T15)	(T15)	(1790)	(3.00)	(2.20)	(0.59)	(0.0026)
				Series III, Tidal Amplitude = 0.10 ft						
28	Side	0	0	0.0037	0.0019	1700	2.83	3.90	0.70	--
19	Side	5.3	0.02	0.0036	0.0019	1740	2.91	3.90	0.70	0.0030
14	Side	29.7	0.02	0.0036	0.0019	1740	2.91	3.90	0.70	0.0030
4	Side	27.3	0.04	(T14)	(T14)	(1740)	(2.91)	(3.90)	(0.70)	(0.0030)
9	Side	27.0	0.056	(T14)	(T14)	(1740)	(2.91)	(3.90)	(0.70)	(0.0030)
25	Bottom	4.9	0.02	0.0034	0.0018	1860	3.08	3.80	0.79	0.0027
24	Bottom	29.7	0.02	(T25)	(T25)	(1860)	(3.08)	(3.80)	(0.79)	(0.0027)
34	Smooth	27.5	0.06	0.0031	0.0010	2010	3.38	3.00	0.94	0.0022
33	Side	Dye	0.02	(T28)	(T28)	(1700)	(2.83)	(3.90)	(0.70)	--

* T = 420 sec.

Table 4

Summary of Diffusion Parameters for Salinity Intrusion

Test No.	s_o ppt	$\dfrac{\Delta\gamma}{\gamma}$	U ft/sec	β t/T	B ft	$\left(\dfrac{s}{s_o}\right)_o$ /min	D_o ft²/sec	D'_o ft²/sec	$\dfrac{D_o}{G^{1/3}}$ (ft)$^{4/3}$	$\dfrac{D'_o}{G^{1/3}}$ (ft)$^{4/3}$	$J \times 10^3$ ft²/sec³	$\dfrac{G}{J}$	$\dfrac{dB}{u_o}$
						Series I, a = 0.05 ft							
18	5.5	0.0027	0.02	0.22	30	0.37		0.41		4.1	0.003	372	0.73
16	29.2	0.0192	0.02	0.28	46	0.62		1.33		13.6	0.019	50	1.12
2	25.6	0.0166	0.04	0.33	60	0.50		2.04		20.8	0.033	29	1.47
11	26.4	0.0172	0.056	0.37	70	0.40		2.46		25.1	0.047	20	1.70
26	28.3	0.0186	0.02	0.27	49	0.66		1.46		15.1	0.018	48	1.05
31	Dye	0	0.02	--	--	--	--		--	--	0	∞	--
						Series II, a = 0.075 ft							
15	29.5	0.0194	0.02	0.26	62	0.58		1.33		10.2	0.019	116	1.10
10	26.8	0.0175	0.056	0.31	83	0.20		1.60		12.3	0.048	46	1.47
32	Dye	0	0.02	--	43	--	0.36		2.8		0	∞	0.76
						Series III, a = 0.10 ft							
19	5.3	0.0026	0.02	0.24	60	0.40		0.76		4.8	0.003	1520	0.90
14	29.7	0.0196	0.02	0.24	62	0.58		1.32		8.4	0.019	202	0.93
4	27.3	0.0178	0.04	--	70	0.26		1.50		9.5	0.035	111	1.05
9	27.0	0.0176	0.056	--	80	0.17		1.70		10.8	0.048	80	1.20
25	4.9	0.0023	0.02	0.17	33	0.43		0.52		3.3	0.002	1670	0.44
24	29.7	0.0196	0.02	0.22	60	0.62		1.45		9.3	0.019	196	0.79
34	27.5	0.0180	0.056	0.25	100	0.35		2.20		15.0	0.053	56	1.12
33	Dye	0	0.02	--	20	--	0.44		2.8		0	∞	0.30